POLYMERIC DRUG DELIVERY OF ANTIEPILEPTIC DRUGS TO NEURONAL NETWORKS CULTURED ON MULTIELECTRODE ARRAYS

By

ALEX JOSEPH CADOTTE

A THESIS PRESENTED TO THE GRADUATE SCHOOL
OF THE UNIVERSITY OF FLORIDA IN PARTIAL FULFILLMENT
OF THE REQUIREMENTS FOR THE DEGREE OF
MASTER OF SCIENCE

UNIVERSITY OF FLORIDA

2004

This document is dedicated to my parents Alfred J. & Frances M. Cadotte.

ACKNOWLEDGMENTS

I would like to thank Dr. Thomas DeMarse for his guidance, patience, and providing a wonderful atmosphere to work in. I would like to thank Dr. William Ditto for his contributions to this project as well as his hard work in building the foundations to what should prove to be a top notch Biomedical Engineering Department. I would like to thank Dr. Chris Sackellares for his many helpful suggestions, references, and knowledge in the field of epilepsy. I would like to thank Penny He for her help with cell preparations and keeping the cell cultures alive which were necessary for this experiment. I would also like to thank my parents, family, and friends for their continued support and encouragement in my return to school for a master's degree.

TABLE OF CONTENTS

page

LIST OF FIGURES

Abstract of Thesis Presented to the Graduate School
of the University of Florida in Partial Fulfillment of the
Requirements for the Degree of Master of Science

POLYMERIC DRUG DELIVERY OF ANTIEPILEPTIC DRUGS TO NEURONAL NETWORKS CULTURED ON MULTI-ELECTRODE ARRAYS

By

Alex Joseph Cadotte

August 2004

Chair: Thomas DeMarse
Major Department: Biomedical Engineering

Neurons in culture fire repetitive synchronized groups of action potentials called bursts. These in-vitro bursts are theorized to be similar to in-vivo epilepsy. Three highly effective anitepilepsy drugs (AEDs) phenytoin, ethosuximide, and valproate were delivered to neural cultures on multi-electrode arrays (MEAs) to determine the extent to which in-vivo epilepsy and in-vitro bursting are similar. A poly-hydroxyethyl-methacrylate (PHEMA) drug delivery ring was developed to deliver these AEDs to the MEAs. The PHEMA rings were found to have no effect on the native activity of neural cultures and proved to be an effective in-vitro drug delivery device. Phenytoin, used for grand mal seizures, was the most effective AED eliminating native and reduced stimulated bursts. Ethosuximide, used for petit mal seizures, and valproate, used for various forms of epilepsy, only slowed the bursting rate and did not prevent stimulated bursts. These findings suggest that bursting in-vitro responds in a similar way to that of in-vivo grand mal epilepsy to these AEDs.

CHAPTER 1
INTRODUCTION AND BACKGROUND

Background

Multi-electrode Arrays

Multi Electrode Array (MEA) technology is used for a variety of different cell cultures. Basically, any cell that creates electrical impulses from ion channel activity can be observed and stimulated on an MEA. These arrays consist of a large number of electrodes embedded into the surface of a specialized culture dish. Figure 1-1 shows an example of a 60 channel (electrode) MEA from Multichannel Systems. Each of

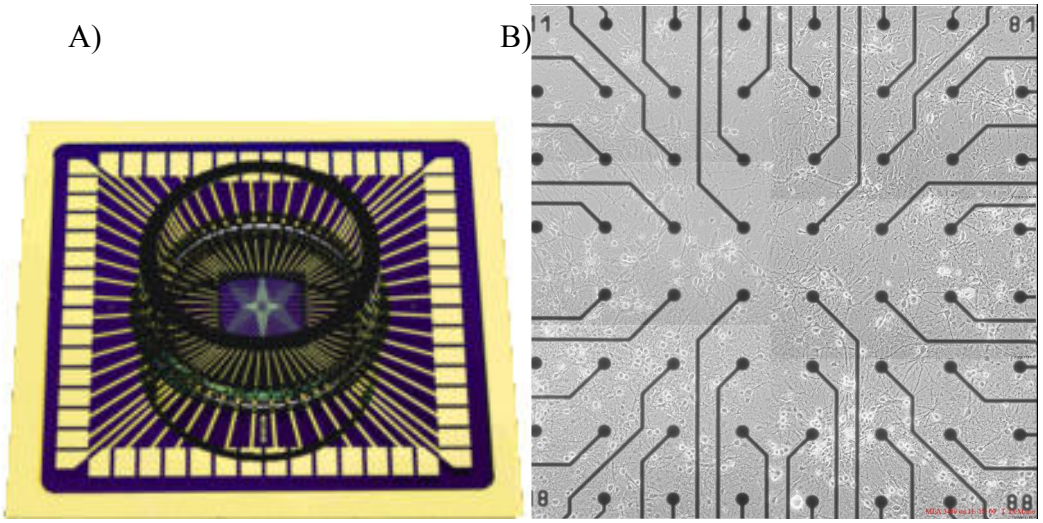

Figure 1-1. Two views of multi-electrode arrays. A) Normal size view of a MEA showing the electrode array inside a glass ring, which is filled with media. The pads around the outside edge of the MEA are connected to individual electrodes within the array at the center of the dish. The MEA is 5cm by 5cm B) Magnified view of the center of the MEA showing the eight by eight grid of electrodes with neural culture present. The point to point spacing of electrodes in the grid is 200µm.

the 60 electrodes can detect the electrical activity, depending on electrode spacing and geometry, produced by action potentials from electrically active tissue growing nearby (Claverol-Tinture and Pine 2002).

Two major neural tissue preparations used on MEAs are slice cultures (Egert et al. 1998; Egert et al. 2002) and dissociated cultures (Tateno and Jimbo 1999). Slice cultures are the preparation of a thin slice of tissue as a relatively intact representation of brain structure. Dissociated cultures are a randomly laid down sample of neurons where structural and connective tissue have been removed via digestion. Figure 1-1B shows an example of a dissociated neural culture on a MEA. Neuronal cultures and hippocampal slices are useful in the study of the electrical behavior of the brain, diseases such as epilepsy, and the effect of drugs on the central nervous system. Much of the research studying these areas has used single electrode patch systems where single neurons among a small population can be studied in detail for several hours. MEA technology was developed in the late 1970's (Thomas et al. 1972; Gross et al. 1977; Pine 1980) allowing the researcher to study the activity of hundreds of neurons simultaneously.

However, there are many more electrically active cells in the human body and other organisms that could be studied on an MEA. For example, cardiomyocytes differentiated from murine embryonic stem cells can be cultured on an MEA (Igelmund et al. 1999). Clusters of these cells form and begin to beat spontaneously and in synchrony depending if pace maker cells are present within a cluster. Once the cell clusters are identified, drugs can be tested in vitro to determine their effect cardiomyocytes activity. The ability and mechanism of toxins that cause an arrhythmia and disturb the electrical coupling between cells have been explored on a cellular level with cardiac cultures grown on a

MEA (Igelmund et al. 1999). Another example is sensory tissues such as photosensitive cells. For example, retinal tissue cultured on MEAs (Meister et al. 1994) has been used to understand how information is processed by the retina into neural signals that are sent to the brain. Retinal tissue responds to photic stimulation in its natural state. When used on an MEA recording is done with the ganglion cell layer. A retina is placed on the MEA with the ganglion layer on the electrodes and optically stimulated and the MEA records the neural response to these stimulations. Understanding the effects of multiple locally applied signals to the intact retinal tissue on image production could help determine mappings for future retinal prosthetics. In short, as long as the cells are electrically active and/or sensitive to electronic potentials, the MEA can be a useful tool for electrophysiology.

The major areas of study using neural culture are neurocomputing, behavioral research, and pharmaceutical research. Companies such as Panasonic developed MEA technology originally for use in neural hybrid computing. Neural computing involves interfacing nonlinear neurons with linear computing to create a new type of computer that could combine the number crunching power of silicon computers with the control and learning capabilities of neural tissue. A great deal of work has been done to understand and make sense of the intact brain and control it for use in computing (Freeman 1994; Gross and Kowalski 1999; Garcia et al. 2002).

Behavioral research centers on the mechanisms and physiology of learning and memory in neuronal networks. The work in this field involves investigating changes in neural networks. Specifically long-term potentiation (LTP) and long-term depression (LTD) both thought to be key to learning and memory in the brain (Tateno and Jimbo

1999; Shahaf and Marom 2001). Stimulation of the culture and feedback from the culture are important to this area of study. Some researchers (DeMarse et al. 2001) have closed this circuit into a control loop with a virtual animal called the Animat with a neural culture brain on a MEA controlling a robotic body.

Pharmaceutical research using MEAs is a new area which has been dominated by patch clamp recordings of single neurons. However, universities, institutes, and major drug companies are beginning to use and this technology for pharmaceutical testing and screening (Moorefield et al. 1999; Egert and Hammerle 2002).

Bursting

Neurons that are cultured on MEAs are spontaneously active, producing stereotyped bursts of synchronous activity across the entire network (Jimbo et al. 2000; Keefer et al. 2001). This synchronized activity is illustrated in the form of a raster plot shown in Figure 1-2 in which activity (action potentials) on each channel (vertical axis) is shown over time. Synchronized bursting appears as vertical groupings points where most of the channels are active. Bursting in these cultures is semi-periodic occurring every 1 to 15 seconds and each burst often lasts from 100 ms to over one second.

During the process of mammalian development there is a period where the network is primarily connected by excitatory synapses. Synchronous bursting behavior is observed in this period or when the inhibitory systems are blocked in adult tissue (Keefer et al. 2001). These bursts have been theorized to be important in the shaping of neural circuits during development (Tosney and Landmesser 1985; Meister et al. 1991). The mechanisms that initiate and terminate a burst are poorly understood. However, the effect of various pharmacological agents on bursting rates and the interval between burst has been studied (Keefer et al. 2001).

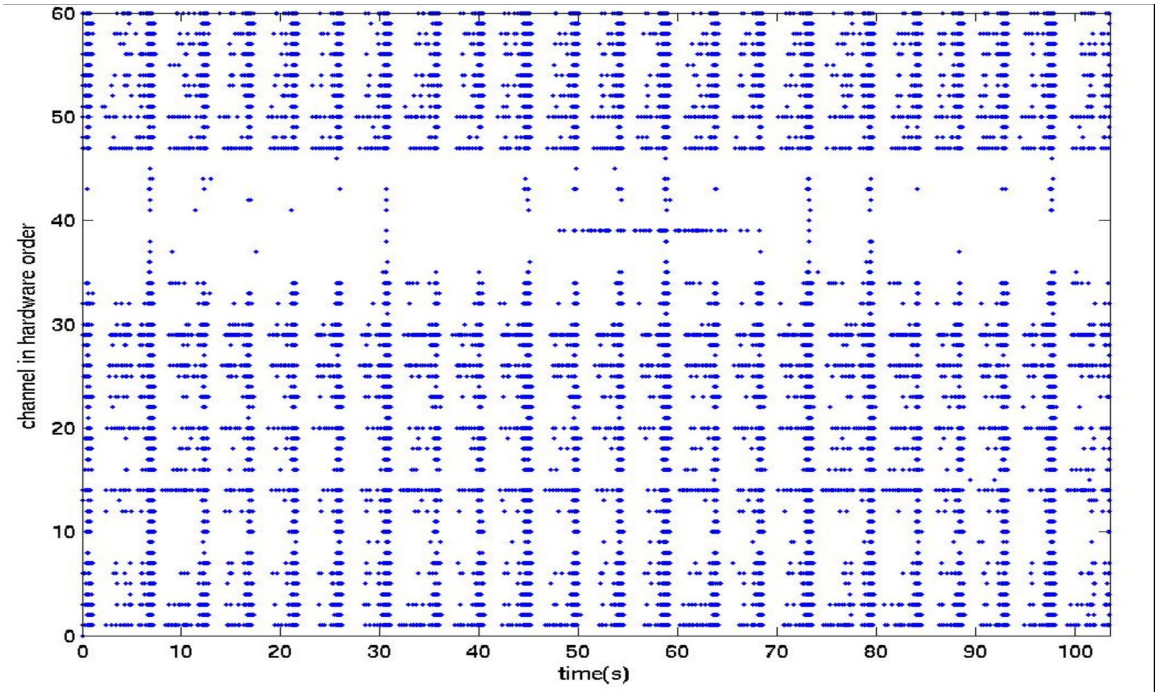

Figure 1-2. This is a raster plot showing neural activity from a dissociated neural culture on a MEA. Time is on the x-axis in seconds and channel number is on the y-axis. The blue dots represent individual action potentials. The vertical groupings of action potentials are bursts.

Epilepsy

Interestingly, spontaneous bursting is reminiscent of patterns of activity found in the intact (in-vivo) brain known as epileptic seizures. A seizure is abnormal electrical activity in the brain that can cause abnormal motor movement, thoughts, and sensations (Brenner 2000). Seizures are the observable symptoms of epilepsy, which can develop as a result of many different origins. These origins include stroke, hypoxia, head trauma, tumors, and many other sources that can alter the function of the brain (Marieb 1998). Often seizures arise from a seizure focus, a group of neurons that elicits a synchronous neuronal discharge, which may then spread from the focus into other regions of the brain.

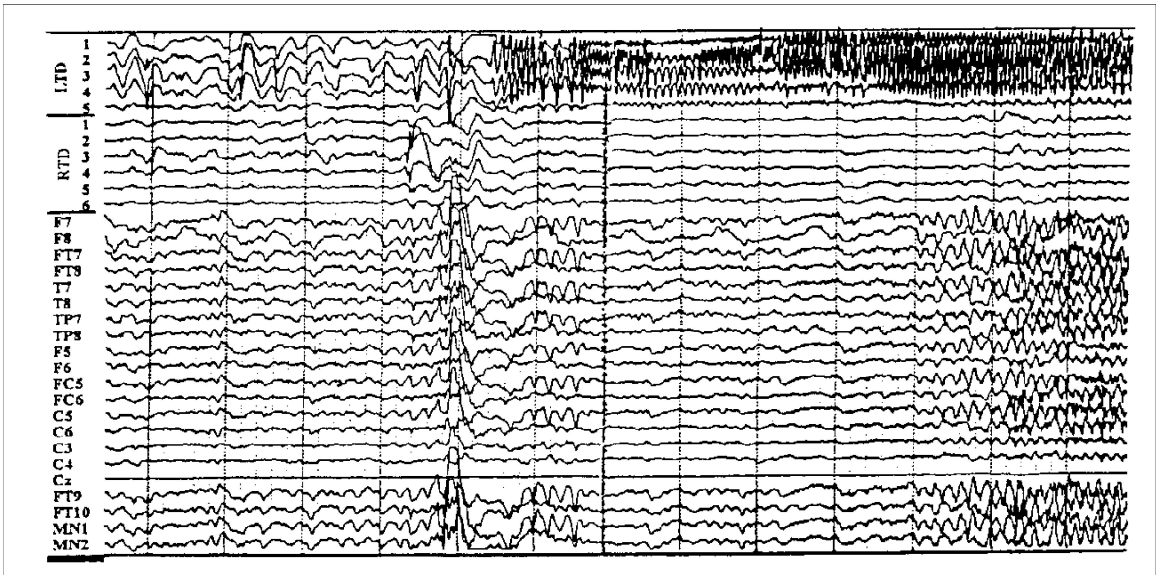

Figure 1-3. This is a representation of a seizure from an EEG from a human epilepsy patient. The top two groups of electrodes are depth electrodes implanted into the patients skull. The remaining electrodes are surface electrodes. The time scale on the x-axis is 1second per division. The seizure onset is at 5s and produces synchronized large amplitude waves of neural activity.

Grand mal and petit mal seizures are two examples of generalized epileptic seizures(Brenner 2000). Grand mal or tonic-clonic seizures are the most well known types of seizures that involve a loss of consciousness and violent muscle contractions and spasms. Petit mal or absence seizures are characterized by a brief loss of consciousness where the subject will appear to be blank or absent with little to no signs of muscle tension or spasms.

Normal and epileptic activity in the brain can be measured using an electro-encephalogram (EEG). The EEG measures potential differences at multiple positions on the scalp on a macro scale through the skull and surrounding tissues. Individual action potentials cannot be resolved but more broad activity patterns at various frequencies can be observed. Figure 1-3 shows a 15 second EEG recording from 25 electrodes located across the surface of the scalp of a human patient (used with permission of the Sackellares Lab).

Polymeric Antiepilepsy Drug Delivery

The Hypothesis

The onset of a seizure begins a few seconds before the appearance of large amplitude waves and continues through the rest of the recording. Both in-vivo epilepsy (Figure 1-3) and bursting (Figure 1-2) represent the onset of coordinated synchronous neural activity and although there are large differences in the duration of each episode, both could be based on a common pathology. In fact, some have hypothesized that the bursting behavior observed in vitro may be epileptiform in nature in both hippocampal slice (Gluckman et al. 1996) and dissociated neural cultures (Segal 1994; DeLorenzo et al. 1998; Egert and Hammerle 2002). For example, Segal suggests that individual neurons in micro-island culture experience epileptiform bursting similar to ictal or interictal activity seen in the hippocampus and neocortex. Segal also references hippocampal slice preparations that have been exposed to low calcium solutions as being epileptic. DeLorenzo varies ion concentrations and adds various bioactive agents while conducting intercellular recordings and calcium imaging in dissociated culture that results in behavior described to be epileptogenic. Egert studies the genesis and spread of epileptic activity in culture. Other experimenters use similar methods to quantify bursting behavior through experiments but stop short of calling it epilepsy (Kamioka et al. 1996; Watanabe et al. 1996; Gross and Kowalski 1999)

Unfortunately, other than these general comparisons, very few experiments have been done to determine if the network activity on an MEA is epileptic or perhaps a part of some other developmental processes such as an arrested developmental state (Meister et al. 1991). This is an important question for those studying neural cultures in vitro

because it would mean that the tissue under study is in a pathological state and could potentially limit any comparisons that might be drawn to normal tissue.

However, there are a number of current pharmacological treatments for epilepsy. If epileptiform activity in-vivo and spontaneous bursting in culture is based on a common pathology, then the prediction would be that the application of anti-epileptic drugs used to prevent seizures in vivo should have similar effects in vitro. This thesis describes a series of experiments to test three of the most common drugs used as anti-seizure medication in-vitro. The drugs used will be phenytoin (used for grand mal seizures), ethosuximide (used for petit mal seizures), and valproate (used for various seizure type including petit mal and grand mal). Each drug will be delivered and tested in-vitro using a novel polymeric delivery system to determine whether they are effective in abolishing in-vitro bursting.

Polymeric Drug Delivery System

One of the challenges of conducting this work, however, is how to deliver these drugs in such a way that these cultures can be studied continuously. For example, one of the most common methods used in vitro is the perfusion system in which a solution is pumped into one side of the MEA and simultaneously removed (via vacuum) on the other. However, perfusion systems are prone to a variety of problems including the possibility of infection, difficulty in setup, leaky tubing, open air chambers, etc. Moreover, perfusion systems are somewhat expensive and not economically practical for all drug delivery applications. As an alternative, a polymeric drug delivery device was developed and tested that is placed in the media of the neural cell culture to dispense the drugs using a concentration gradient. This monolithic device is made of poly hydroxyethyl methacrylate (PHEMA), a hydrogel often used to make contact lenses

(Ratner 1996). The production costs of these small polymer devices are minimal. The PHEMA ring was tested in the first phase of this project for toxicity and it's diffusion capabilities were tested before testing anti-epilepsy drugs. The second phase of the project will used these rings to deliver and test the efficacy of the antiepilepsy drugs.

CHAPTER 2
DEVELOPMENT OF THE PHEMA MEA DRUG DELIVERY SYSTEM

Poly Hydroxyethyl Methacrylate Background

Hydrogels are cross-linked polymeric structures that can become swollen with water. These polymers are made up of monomers that by chemical reaction have been polymerized into long chains connected in a macromolecular network, similar to a dense spider web. Hydrophilic or water loving monomer is used so that the resulting polymer has an affinity for water.

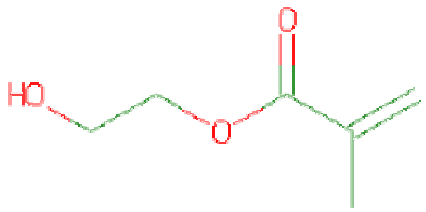

Figure 2-1. The hydroxyethyl methacrylate monomer. The carbon-carbon double bond in the top left opens up to form a vinyl linkage that forms the backbone of the Poly-HEMA molecule.

Acrylic acids have been used to make polymers for biomedical applications such as intraocular lenses since World War II (Ratner, 1996). As hydrogels for drug delivery their uses have been extensively studied and documented(Ratner 1996; Hoffman 2002; Nuttleman et al. 2002). Poly hydroxyethyl methacrylate (PHEMA) is an acrylate polymer made from the HEMA monomer shown in Figure 2-1. It is a commonly used biomedical hydrogel. PHEMA has been a notable material in this class of polymers due to the fact that when fully swelled it has a similar density and water composition to that of living tissue. PHEMA is biologically inert, nonionic (suitable for blood contact), resists

degradation, is permeable to metabolites, non-absorbable, can withstand autoclave sterilization and can be molded to most any shape. Acrylates along with PHEMA are also optically clear. As a biomedical polymer, these properties have been taken advantage of for use most notably in contact lenses for the correction of vision (Ratner 1996).

Pharmaceutical applications for hydrogels including PHEMA have become a topic of much investigation over the past fifteen years. The basic principle is to dissolve a water-soluble drug in solution that is absorbed by the hydrogel. When placed into an environment that lacks this agent a concentration gradient is formed and allows for outward diffusion of the drug into the surrounding environment(Ratner 1996).

PHEMA is useful for use in delivering pharmaceutical agents to neural cultures due to it's non-toxicity, inertness, optical clarity, and ability to absorb and release pharmaceutical agents and metabolites. Ideally any material that is introduced into a neural culture during an experiment should do nothing to disturb the native activity of the culture. Ideally, only the agent that it carries should have an effect on the culture. Many variables must be observed to insure no interactions occur when the PHEMA is placed in the culture dish. The medium the PHEMA is soaked in must be the same temperature, concentration, and gas content as the medium. Changes in the ionic concentrations of the medium for example can change the behavior and firing rate of neurons (Hille 1992). The PHEMA must be sterile, fully polymerized, clean, and carefully placed into the dish to prevent contamination or agitation of the culture.

The initial testing of this material in neural culture was to simply test for acute and chronic toxicity. Over the course of two weeks five control dishes were visually compared to five dishes with sterile prepared PHEMA slabs added to the medium. In all

dishes there were no signs of acute or chronic toxicity. Even in cases where the PHEMA slab was directly on top of the neural culture the cultures showed no signs of toxicity. This case also demonstrates permeability similar to water of the PHEMA to dissolved gases and metabolites in the medium.

Design, Fabrication, and Use of the PHEMA Drug Delivery Ring

Design and fabrication of the PHEMA ring for use in a neural culture on a MEA was carried out to ensure repeatability, sterility, and material purity. The ring was designed to be smaller in diameter, when swollen, than the inner diameter of the MEA dish. The device is a ring rather than a disk to prevent the material from actually touching the culture in the middle of the dish. This prevents abrasion of tissue from the culture and prevents the PHEMA from influencing dissolved gas transport to and from the culture.

The specific recipe for the PHEMA used in this experiment is adapted from the laboratory section of Dr. Goldberg's Polymeric Biomaterials class (Goldberg 2002). The major changes to this method include the use of a Teflon mold specific for creating rings and the use of sterile procedures to ensure purity and sterility. To create the material used in these experiments 4mL of ultra pure tissue culture water and 7.5 grams of 2 2'-azobisisobutyronitrile (AIBN) initiator was added to 4mL HEMA monomer in a 50mL test tube. The reaction mixture was blended by shaking and then pipetted as needed into the sterile Teflon mold. The mold was then placed in an oven at 90C to 95C for 1 hour to allow for polymerization. The smell of the monomer from the mold indicates that a longer baking time is required. At lower temperatures the reaction will not occur and at temperatures above 100C the PHEMA will develop bubbles in the solid that interfere with the rings homogeneity.

After removal from the oven the PHEMA ring is ready to be removed from the mold. If allowed to cool the PHEMA will become brittle and will be difficult to remove from the mold. Cool the top of the PHEMA ring by filling the mold with sterile culture water while the ring is hot and in a sterile environment. Immediately use a pick to impale the ring and pull it from the mold. This should be easy if the ring did not cool for too long. If the ring is brittle or cracks one solution is to try putting the ring back in the oven with a little water to soften the ring. Once removed the ring was placed in a sterile 50mL test tube and sealed for later use. An example of a freshly molded ring, a used ring, and their Teflon mold is shown in Figure 2-2. The rings can be kept in this sealed sterile environment for an indefinite amount of time until hydrated for experiments.

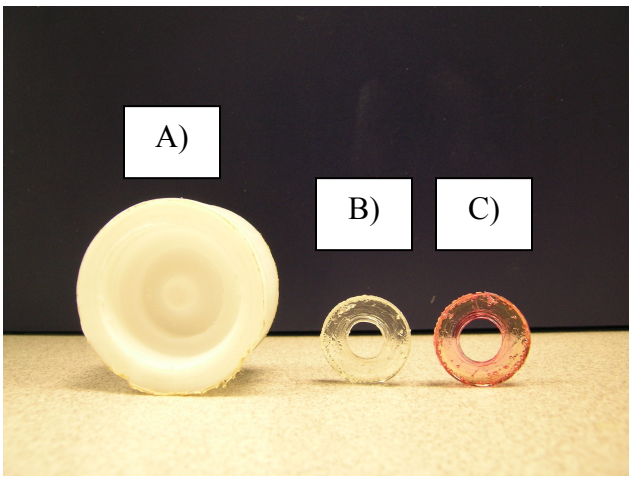

Figure 2-2. Teflon mold and new and used PHEM rings A) The Teflon mold that is used to create PHEMA rings. B) A freshly created PHEMA ring removed from the mold. Notice the optical clarity and rigidity of the ring. C) A used PHEMA ring that has been soaked in a medium and drug solution and used to deliver the drug to a neural culture.

When used in an experiment the PHEMA ring must be hydrated in fresh medium in an incubator to allow carbon dioxide concentration and temperature of the ring to reach equilibrium. Figure 2-2C shows a ring that has been soaked in medium as shown by its

red color. Sufficient time must be allowed for the equilibrium water content of the PHEMA to be reached. It is recommended to prepare the rings with medium a few hours before an experiment. Pharmaceutical and bioactive agents should be added at this time to allow for the agent to soak into the PHEMA hydrogel. While placing the PHEMA ring into an MEA culture dish care must be taken not to touch the neural culture and to use sterilized forceps. The outer surface of the ring was rinsed with medium to remove surplus liquid and to prevent delivery of excess pharmaceutical agent from the surface of the material.

Several problems may emerge from incomplete polymerization of the HEMA (the monomer is toxic) or non-optimal crosslink density of the polymer. Incomplete polymerization could result from not baking the HEMA long enough to fully polymerize the monomer. Preliminary testing has shown that baking at 90C results in a good polymerization without damaging the resulting polymer. Crosslink density is controlled directly by the amount of cross-linking agent added to the reaction mixture (Goldberg 2002). If the crosslink density is too high then the rate of diffusion into and out of the PHEMA will decrease to the point where the PHEMA would be nonfunctional as a drug delivery device.

The PHEMA rings were tested in-vitro for toxicity, effects on the activity of neural culture, and basic functionality before they were used to deliver antiepilepsy drugs to neural cultures. Chapter 3 describes the materials and equipment used to culture, maintain, and record from neural cultures on MEAs. Understanding these principles and the equipment used allows one to better understand the reasons for and the process of testing PHEMA ring in-vitro, which will be discussed in Chapter 4. This testing will

insure that when the antiepilepsy drugs are delivered using the PHEMA ring, any effects will be a result of the drugs and not the PHEMA alone.

CHAPTER 3
MATERIALS

Cell Culture

Dissociated Neural Cultures

Cortical tissue from E17 – E18 Wistar rat embryos (Brain Bits Inc.) was digested using the Papain Dissociation System (Worthington Biochemical Corporation) and mechanically triturated separating the neuron's soma from the surrounding connective tissue. The resulting suspension of cells consists of both neurons and glia. Immediately after plating the neurons on an MEA they appear as small spheres with a dark center.

After dissociation, approximately 50,000 cells are placed in the center of a multi-electrode array that has been coated with polyethyleneimine (PEI) (Lelong et al. 1992) and laminin (Sigma) (Banker and Goslin 1998). The PEI creates a surface that is hydrophilic and favorable to the growth of neurons. Laminin is a component of the extracellular matrix of the neurons and serves as a building material for the neurons to bind to the surface and grow axons and dendrites. Having the laminin present allows the neurons to mature faster. If the surface treatment is not favorable the neurons may be more attracted to each other rather than the surface. This will lead to clumping of the neurons into small islands, which would limit the electrical contact and number of active electrodes.

Medium is required to feed the neurons in an ex-vivo environment. It mirrors the content of blood as far a proteins and nutrients. The neurons are cultured in medium consisting of 90% Dulbecco's modified Eagle's medium (DMEM) (Gibco cat# 10569-

010) and 10% Equine Serum (HyClone cat# SH30074.03). The medium is allowed to equilibrate to 5% carbon dioxide and 35C temperature in an incubator before use. Medium is changed twice a week or as needed.

Development of Culture Activity

The neurons begin to connect to each other by regrowing their axons and dendrites within the next few days after plating. Action potentials from these neurons can be detected within this time. Over the next two weeks the embryonic cells begin to express their ion channels. The excitatory N-methyl-D-aspartate (NMDA) ion channel system matures quickly within the first 3 to 8 days postnatal. The excitatory systems are thought to be responsible for epileptiform bursting behavior(Bugard and Hablitz 1993; Keefer et al. 2001). The inhibitory gamma-amino butyric acid (GABA) ion channel system develops and begins expression within the first 6 to 10 postnatal days (Luhmann and Prince 1991). Inhibitory systems are notably absent for the first postnatal week. For dissociated culture this translates into maturity being reached within the first four weeks. Figure 1-1B shows an example of a mature neural culture. Experiments are typically carried out with active mature cultures only past the 30-day post natal age to prevent interference from the maturation process.

Hardware and Software

The Multi-electrode Array

The multi-electrode arrays used in the DeMarse lab are purchased from Multichannel Systems (cf. Figure 1a and 1b). The electrodes are arranged in an eight by eight grid with the corners missing giving a total of 60 electrodes. Each electrode records the electrical activity produced by nearby neurons as they fire action potentials. These electrodes can also be used to stimulate activity by applying a bi-phasic voltage pulse

(100 to 800 mV) through an electrode, which causes neurons near the electrode to fire. Hence, these arrays can be used to both measure and stimulate the ongoing neural activity of a small population of neurons or other electrically active tissue.

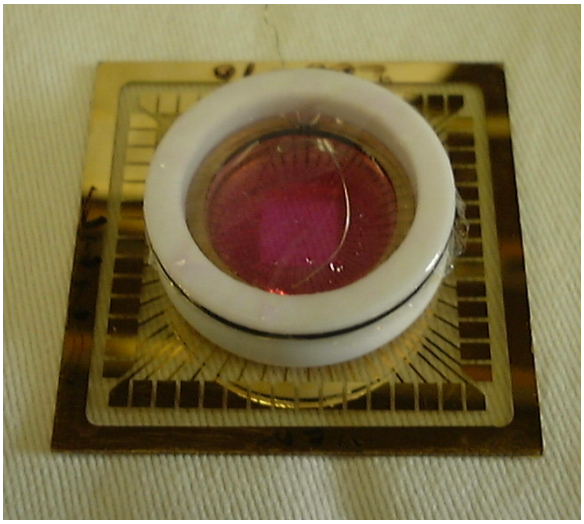

Figure 3-1. This is a multi-electrode array with a white Teflon lid with the FEP Teflon membrane attached. This effectively seals the culture from infectious agents keeps moisture in the dish, and allows for gas transport across the membrane.

Culture System

Neural tissue is sensitive to infection by mold, yeast, and bacteria. Specialized lids have been designed (Potter and DeMarse 2001) that are made of a Teflon ring that seals around the base of the dish and at the top allows for a FEP Teflon film to be attached. Figure 3-1 shows an example of an MEA with a Teflon lid with the FEP membrane attached. This FEP covering allows for carbon dioxide and other gases to pass through while preventing water and contagions from getting in or out. This effectively seals the culture from infectious agents and retains water to prevent hyperosmolarity from the evaporation of water in the medium. When used properly they can extend the lifetime of a culture to as much as two years.

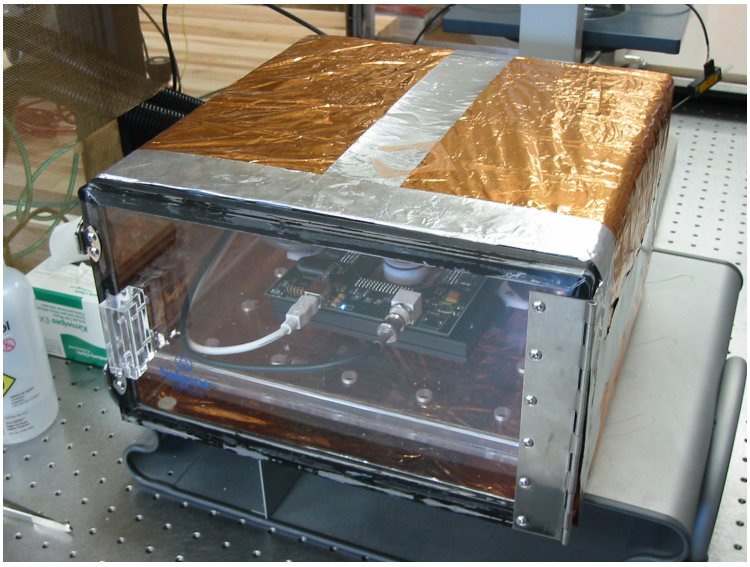

Figure 3-2. The micro-incubator constructed to control the environment around the MEA-60 and the neural culture during experiments. The temperature, humidity, and carbon dioxide concentrations are all controlled inside the enclosure.

Physiological Environment

The environment around the MEA60 is temperature and gas compositionally controlled. The MEA 60 is temperature controlled using the Multichannel Systems TC02 temperature controller. Air temperature and carbon dioxide content are controlled by creation of a mini incubator around the MEA60 shown in Figure 3-2. In this case an acrylic desiccators has been converted to house the MEA60 with an access door and input/output ports for temperature controlled air, carbon dioxide, and electrical wiring. This setup is wrapped in conductive foil to reduce heat loss. The temperature and carbon dioxide controllers were made in the DeMarse lab specifically for this application.

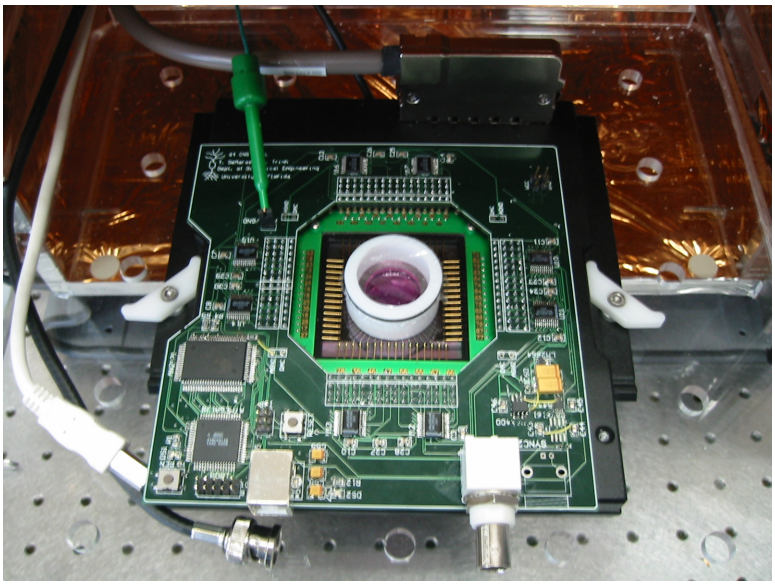

Figure 3-3. The MEA-60 from Multichannel systems with the 64 channel stimulator attached. A MEA with it's Teflon lid is in the apparatus.

Data Acquisition System

The connection to the MEA dish is provided by the MEA60 amplifier system also made by Multichannel Systems. This allows for a cable connection to the MC_Card, which is a 64-channel analog to digital (A/D) card for data acquisition that fits into a PCI card slot in a PC. Stimulation is provided to the dish by a 64-channel stimulation board that attaches to the top of the MEA60. This stimulation board was developed and built in house by Dr. Tom DeMarse and Vihn Trinh. These components are shown in Figure 3-3. Raw electrical activity is recorded at 25kHz per channel. Since, a typical action potential is approximately 1ms long this system provides more that adequate resolution to measure the wave form. The MEA60 system consists of three distinct parts. An amplifier to amplify neural signals whose amplitude typically ranges from 20□V to over 100□V. The data is digitized using an in host data acquisition card (PCI interface) capable of bus

mastered transfer to main system memory at 3.3 MB/sec. The host computer can then perform analyses (e.g. spike detection, artifact suppression) that are required.

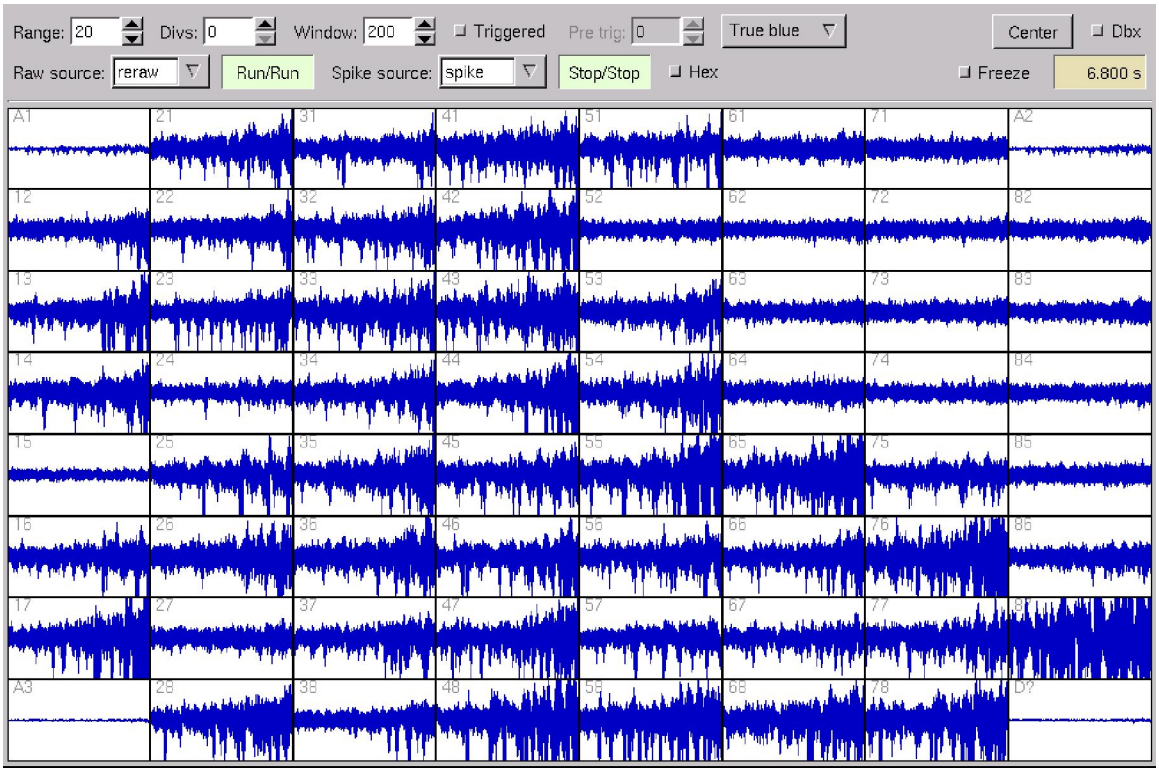

Figure 3-4. Raw electrical activity from a neural culture on an MEA. The large deviations seen in the individual boxes represent action potentials occurring near the corresponding electrode on the MEA. This picture shows the raw activity of the culture during a burst. For each window voltage is represented on the y-axis and time (approximately 200ms) on the x-axis.

As mentioned previously, raw electrical activity is sampled at 25KHz on each channel and digitized (12 bit). For each sample the 64 available channels are sampled in hardware order around the outside of the MEA dish instead of any geometric pattern. A map of the hardware order to the geometric channel locations is necessary to determine the location of a channel in the MEA dish as the data is recorded in hardware order. Culture electrical activity is then viewable and is processed in real time on the computer monitor. An example of this activity is shown in Figure 3-4. The raw data can then be

streamed in real-time (low latency) to other machines via a dedicated TCP/IP 1GB ethernet for further processing, analysis, or stimulation.

Spike and Burst Detection Algorithms

Raw data from the MEA is available to the computer at 25kHz for 64 channels. For the most part the bulk of this data is not spike information. A raw recording of this magnitude could take up 3.3 megabytes of storage per second. This file size becomes unwieldy when 20 minutes of data are recorded, 3.5 gigabytes in this case. To prevent such large file sizes and to eliminate data that is not relevant to spiking events, only the spike events were recorded. The MEABench (written by Daniel Wagenaar) software is a set of command line and GUI utilities to process data from the MEA60. This software is used in these experiments to visualize, process, and record data. Each recorded spike event contains information about the time (at peak), channel, height, width, threshold used, and one ms of context raw data around the peak time. Spikes are detected in real time via a moving voltage threshold based on 5 standard deviations of the noise.

This spike file is later processed offline to extract information about any bursts that may have occurred. The burst detection algorithm, which was developed in MATLAB, is shown in Appendix A. This algorithm uses a leaky integrator to determine when temporally related spiking events constitute the beginnings of a burst. This algorithm is an adaptation of a method described by Gross (Stenger and McKenna 1994). Gross' algorithm uses the difference between two leaky integrators to determine the threshold for entering into and exiting the bursting condition. The end of a burst is characterized by a period of inactivity with no spiking similar to the refractory period for individual neurons. Instead of using the same leaky integrator to exit the bursting condition this algorithm searches for this period of inactivity to establish the end of the burst. The burst

start and stop time are recorded. This algorithm also calculates the burst duration and the interburst interval (the time between bursts) along with statistical information such as standard deviation for these measures. These measures will be critical for measuring changes in culture activity in the following chapters where the PHEMA ring and eventually antiepileptic drugs will be tested in-vitro.

CHAPTER 4
TESTING OF THE PHEMA MEA DRUG DELIVERY SYSTEM

Testing the PHEMA-MEA system with bicuculline

A series of experiments was conducted to determine the effect of the poly HEMA ring on the activity of neurons cultured on a MEA and the effectiveness of the drug delivery device in general. It was first important to determine that the poly HEMA ring alone does not have an effect on the normal electrical activity of the neural culture. Test of the ability of the ring to delivering bioactive agents was conducted using bicuculline, which produces a well known stereotypic response in neural culture.

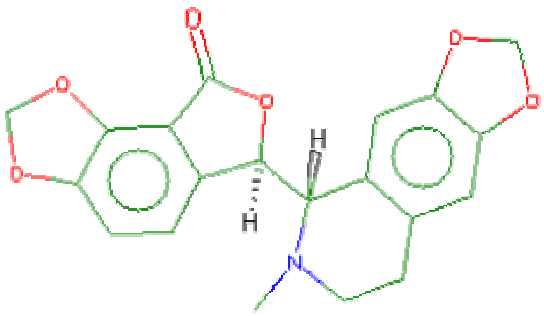

Figure 4-1. The chemical structure of bicuculline, a bioactive agent derived from *Dicentra cucullaria.* Bicuculline is a pro-convulsive agent that evokes rhythmic bursting from neural cultures.

Bicuculline shown in Figure 4-1 is a phthalide isoquinoline a bioactive agent derived from *Dicentra cucullaria* a flowering plant common in North America. Manske first isolated it in 1932. Bicuculline is a specific competitive agonist of GABA (Razet et al. 2000). When applied to neurons ex-vivo stereotypic rhythmic bursting behavior results (Stenger and McKenna 1994). Bicuculline, when applied to neural culture on an

MEA, has been shown by Keefer to result in increased burst durations (Keefer et al. 2001). Direct injection of bicuculline into the motor cortex of monkeys produces rhythmic dystonia which is characterized by involuntary muscle contractions that cause involuntary movement and twisting of body parts (Guehl et al. 2000).

Experimental Procedure

First, ten-minute baseline recordings of neural activity from four MEAs were conducted without HEMA rings. This baseline data will be compared to the neural activity in the presence of a HEMA ring with and without bicuculline. The primary measures of neural activity were interburst interval (IBI) and burst duration (BD). IBI is a measure of the time between bursts while BD is a measure of the duration of a burst. The maximum intensity of the burst (determined by maximum average firing rate during the burst) will also helpful in characterizing bursting behavior.

Following baseline experiments, a placebo poly HEMA ring soaked in medium and equilibrated in a 5% CO2 incubator, was placed in each of the MEAs and activity will be measured for 10 minutes. A placebo was conducted to insure that the PHEMA with fresh media does not have an effect on either burst or firing rates.

Data from the placebo will be compared to cultures in which the PHEMA ring has been soaked in 100μmol/L bicuculline. Bicuculline removes inhibitory mechanisms from the neurons and should create a highly stereotypic periodic rapid burst (Moorefield et al. 1999). Bicuculline induced burst activity was recorded and compared to control (native) and placebo activity. The MEAs were then rinsed with media to remove the bicuculline and placed in the incubator for later use.

PHEMA Bicuculline Testing Results and Discussion

Application of the placebo ring produced no apparent effect on burst activity relative to baseline recordings. In contrast, rings with bicuculline showed substantial increases in burst duration and interburst interval.

Figure 4-2 shows the burst durations for the bicuculline treatment for four dishes in baseline, placebo, and bicuculline conditions. The placebo and baseline conditions do not show appreciable differences in mean or variation suggesting that the PHEMA has little effect on burst duration. The mean burst duration increases greatly when comparing bicuculline treatment to baseline, while the variation stays relatively the same.

Figure 4-3 shows the interburst interval for bicuculline treatment for the same four dishes in baseline, placebo, and bicuculline conditions. The placebo and baseline conditions do not show any significant changes in the mean or variation of interburst interval suggesting that PHEMA has little effect on interburst interval. The mean and variation of interburst interval increase when comparing bicuculline treatment to baseline.

Figure 4-4 shows a raster plot with the neural activity for culture 6682 during the ten-minute baseline, application of the placebo ring, and application of a ring with bicuculline. The bicuculline raster plots for the remaining cultures are in Appendix B. The changes in burst duration and interburst interval are plainly visible when comparing baseline and treatment runs while baseline and placebo runs look very similar.

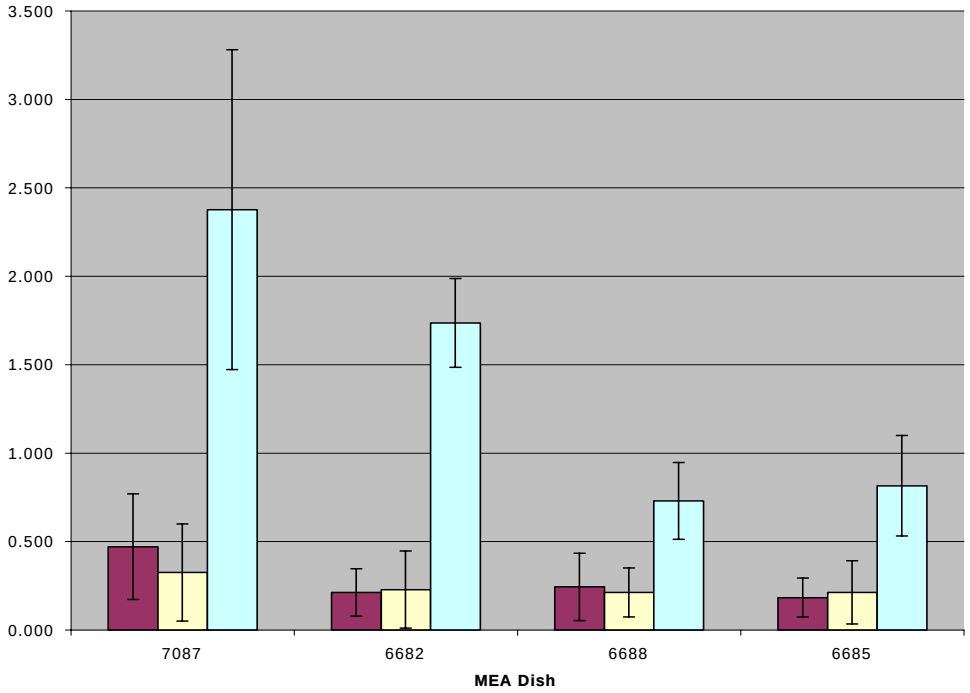

Figure 4-2. Bicuculline average burst duration. Mean burst duration during baseline, placebo, and bicuculline treatments.

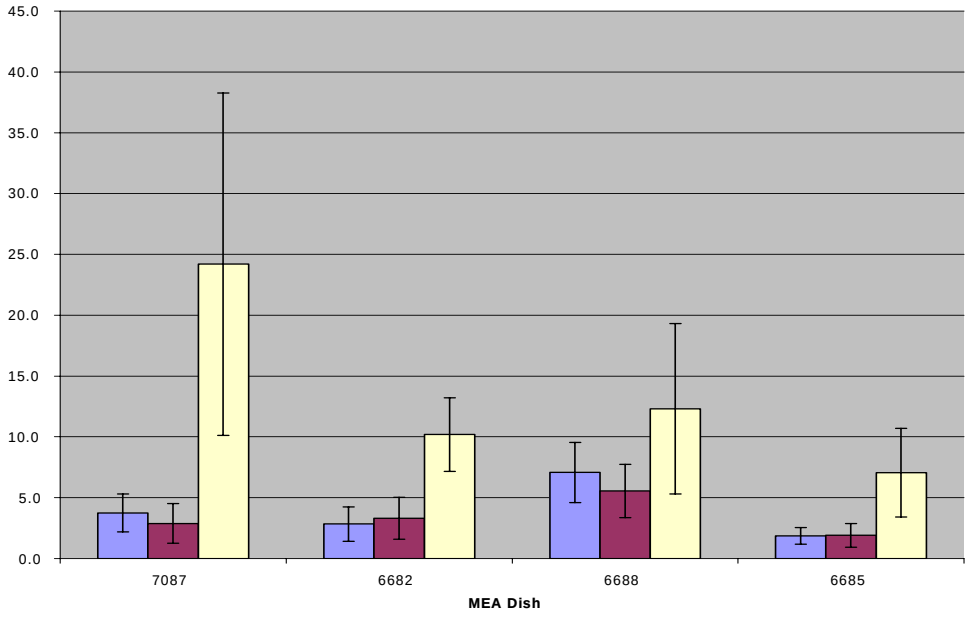

Figure 4-3. Bicuculline mean interburst interval. Mean interburst interval in seconds (y-axis) during baseline, placebo, and bicuculline treatments for four MEAs (x-axis).

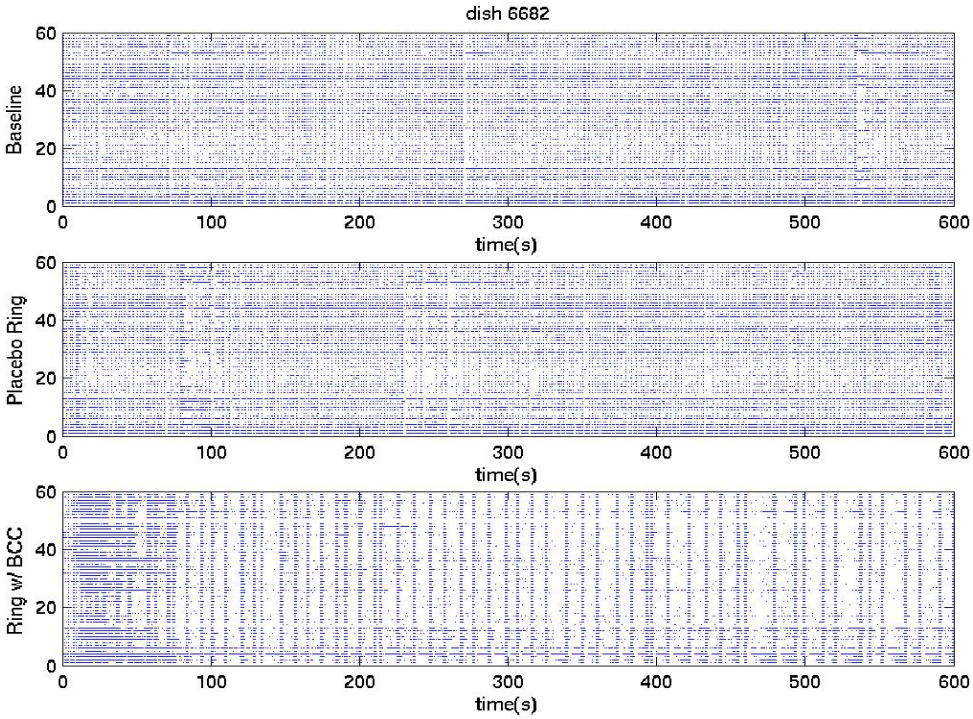

Figure 4-4. Raster plots of spike activity for dish 6682 during baseline, placebo, and bicuculline treatment spike activity. Time is on the x-axis in seconds and channel in hardware order is on the y-axis each point represents an action potential from a nearby neuron.

Bicuculline when applied to the culture with a PHEMA ring tended to increase the mean interburst interval and the mean burst duration in each case. Variation overlapped for dish 6688 but the mean increases as it did in the other cultures. This difference can be seen graphically for interburst interval in figure 4-2 and BD in figure 4-3. The effect of the bicuculline on the burst duration is consistent with those of Keefer (Keefer et al. 2001) in that the burst duration significantly increased. The IBI grew longer where Keefer shows no major change in burst rate with bicuculline. Keefer measures the burst rate rather than interburst interval, which are inversely related.

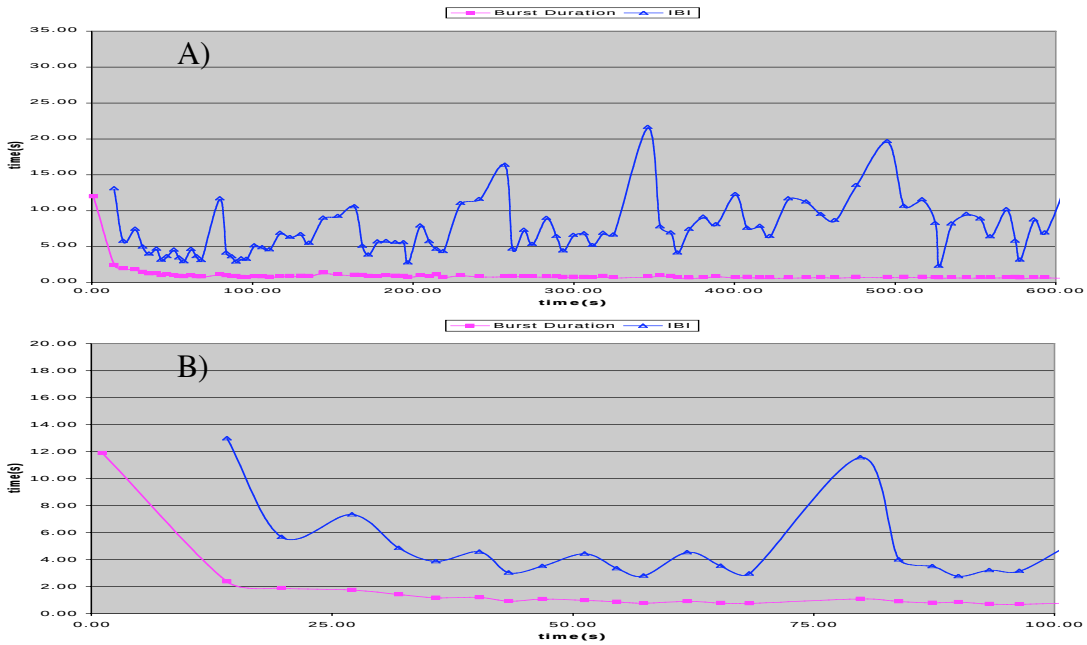

Figure 4-5. Dish 6685 with a standard concentration of 100mmol/L bicuculline. A) The full 600 seconds of treatment B) The first 100 seconds of treatment. These plots shows the almost immediate effects of bicuculline on the culture at this concentration.

Application of bicuculline showed an effect within the first ten seconds at this high concentration such as in Figure 4-5 A & B. One might expect to see a gradual change in burst characteristics as the drug diffuses out of the ring. However, the effect in this experiment at this concentration occurred within the first 10 seconds. The relatively high concentrations of bicuculline used show no such release rate shown by a slow activity change but rather a fast abrupt change. Two cultures were tested at a much lower concentration, 10mmol/L bicuculline, to assess whether concentration has an impact. Figure 4-6 shows the effect of a PHEMA ring soaked in 10mmol/L bicuculline. The IBI gradually increases until around time = 40s where the major effects of BCC can be seen with increased BD and IBI. This shows that the BCC is released slowly from the PHEMA ring. Both the interburst interval and burst duration during the first 40 seconds following the application of the drug gradually increase. However at 40 seconds there is

an abrupt increase in BD and IBI. This effect would be expected due to the first order release rate from the monolithic PHEMA (Ratner 1996).

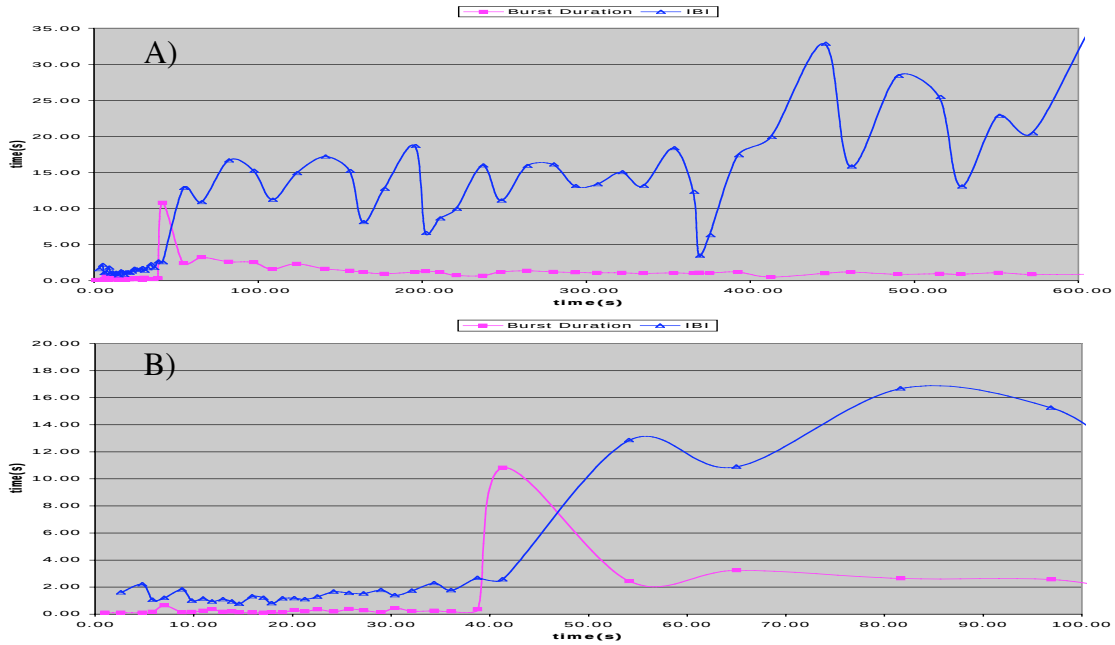

Figure 4-6. Dish 6685 with a concentration of 10mmol/L bicuculline. A) The full 600 seconds of treatment B) The first 100 seconds of treatment.

Conclusions

One dish was killed immediately due to a rough edge on the PHEMA ring that accidentally removed the culture from the dish surface. This was corrected by increasing the inner diameter of the PHEMA ring to help prevent contact between the PHEMA and the neural culture. When the ring was not removed properly the edges of the culture can be disturbed and leading to peeling of the culture from the edges. This peeling will eventually remove the culture from the surface.

Overall the PHEMA ring performed as anticipated as a drug delivery device. The bicuculline was absorbed into the polymer matrix and released over time. There was no evidence of infection or contamination due to the use of the rings. In the few cases that a failure occurred the cause was primarily poorly made rings that physically abraded and

damaged cultures. This was remedied by making the inner diameter of the rings larger. When manufactured correctly in a sterile environment the PHEMA drug delivery ring proves a viable cost effective alternative to a perfusion system for drug delivery. These rings were used for all future drug delivery in this project.

CHAPTER 5
ANTIEPILEPSY DRUG TESTING

Antiepileptic Drugs

If bursting originates from the same mechanisms antiepilepsy drugs should have a similar effect on in-vitro bursting as they do in-vivo epilepsy. Three antiseizure drugs were chosen for testing. They were: phenytoin, ethosuximide, and valproate. Each was delivered to the cultures using the previously tested PHEMA drug delivery device. Each of these drugs has been in documented use for treatment of epilepsy for many years (Brenner 2000; Levy et al. 2002).

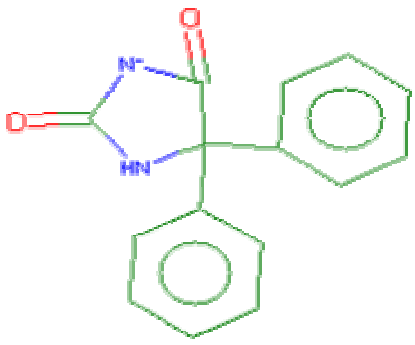

Figure 5-1. The chemical structure of phenytoin. Phenytoin is a white powder that dissolves in a basic aqueous solution. As a antiepilepsy drug it is mainly used for grand mal seizures.

Phenytoin

Phenytoin shown in Figure 5-1 is a hydantoin derivative used to treat partial seizures and generalized tonic-clonic seizures (Brenner 2000). Merritt and Putnam first used it in the treatment of epilepsy in 1938 (Levy et al. 2002). It was the first anticonvulsant that does not result in sedation of the patient. Its major method of action

is blockage of voltage sensitive sodium channels in a neuron's cellular membrane. The spread of electrical discharge from a seizure focus to the surrounding tissue is though to be reduced by this effect, as the neuron is no longer as voltage sensitive. The therapeutic serum concentration is 10 - 20 ug/mL (Brenner 2000).

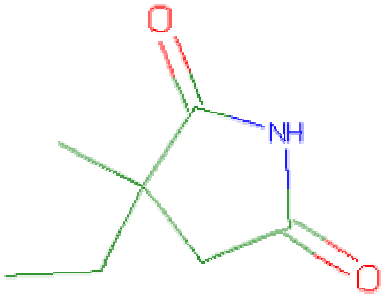

Figure 5-2. The chemical structure of ethosuximide. Ethosuximide is a nonionic white powder that dissolves in ethyl alcohol. As a antiepilepsy drug it is mainly used for petit mal (absence) seizures.

Ethosuximide

Ethosuximide shown in Figure 5-2 is a succinimide derivate that is used primarily in the treatment of generalized absence or petit mal seizures (Brenner 2000). Its primary effect is thought to be on the T type calcium channels that regulate the entrance of calcium into the neuron. It has many other effects and has proven to be difficult to isolate its anticonvulsant actions experimentally. It is known not to have any effect on voltage sensitive sodium channels like phenytoin and other antiepileptic drugs (Levy et al. 2002). The therapeutic serum concentration is 40 –100 ug/mL (Brenner 2000).

Valproate

Valproate shown in Figure 5-3 is a branched chain fatty acid with a relatively low molecular weight. Its mechanism of action is wide and is effective on many types of seizures including both generalized and focal types (Brenner 2000). It has been shown to

block not only voltage sensitive sodium channels but also increases GABA production and slows degradation of GABA. No single effect of valproate can be claimed to be it's primary mechanism of action as the efficacy of its antiepileptic inhibition is broad(Levy et al. 2002). Valproate has also been shown to prevent rapid firing of action potentials of CNS neurons in culture(Levy et al. 2002). The therapeutic serum concentration is 50 - 100 ug/mL (Brenner 2000).

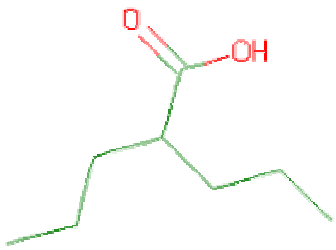

Figure 5-3. The chemical structure of valproate. Valproate is a clear crystalline solid that dissolves easily in aqueous solution. As an antiepilepsy drug its uses are wide including both petit mal and grand mal seizures.

The three drugs were chosen because they represent a good spectrum of common antiepileptic drugs. Phenytoin is primarily for grand mal seizures, but has also been found to increase absence seizure activity. In contrast, ethosuximide is mainly used to treat absence seizures while valproate can be used in the treatment of a wide variety seizure types. Due to their differing methods of action there would be potential differences in their effects. For example, if bursts in-vitro resemble grand mal seizures then phenytoin should be effective in attenuating or even removing bursts while ethosuximide would not.

Experimental Procedures

A PHEMA drug delivery ring was prepared, as discussed previously, prior to each experiment. After polymerization the PHEMA ring was soaked overnight in a media and

drug solution to thoroughly hydrate and saturate the PHEMA. This was conducted in the incubator with a FEP Teflon lid on the container to allow equilibration of CO_2, O_2, temperature and pH to match that of the media in the MEA dishes.

Phase 1: Effects on Spontaneous Changes

Phase one of the procedure tests the change in interburst interval and burst duration when the cultures are exposed to the antiepilepsy drugs. The MEA cultures were individually removed from the incubator and placed in the test rig. The test rig acts like an incubator maintaining a similar temperature and carbon dioxide concentration as that of the incubator. Four MEA cultures were used for experiments for each drug. Baseline recordings were conducted for all dishes pretreatment and post-wash. The PHEMA ring was removed after each treatment and the MEA was rinsed with media in a series of five washes to remove the residual concentrations of the drugs. A typical experimental session began with 10 minute baseline spike recordings. This baseline data was compared to the treatment and return to baseline recordings. The treatment for each dish begins after baseline recordings when a drug laced PHEMA ring was placed into the MEA. Treatment recordings will be 20 minutes duration. The dish was then washed five times with medium after removal of the PHEMA ring. Return to baseline recordings repeat the same ten-minute recordings to match the baseline.

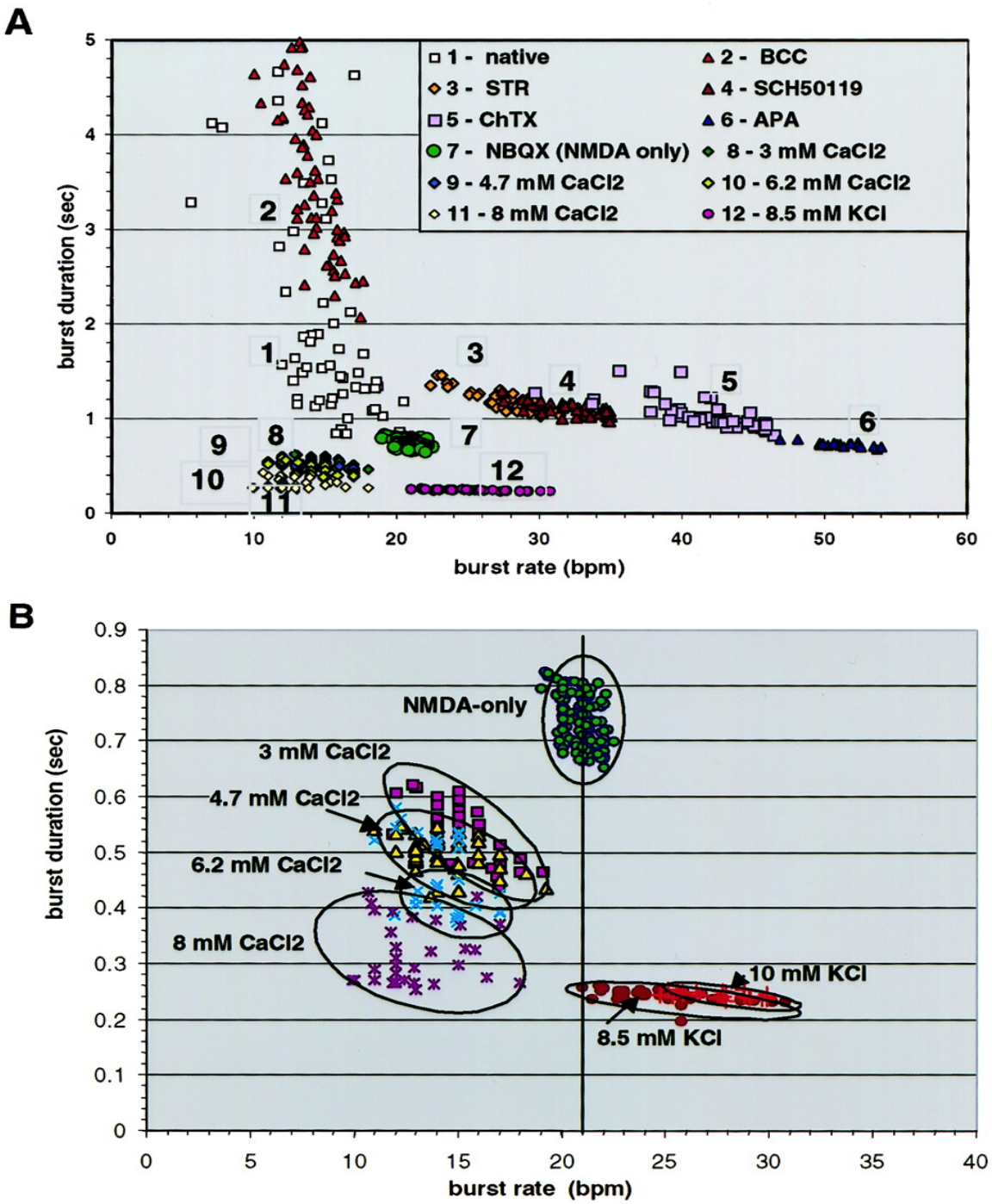

Figure 5-4. Figure 8 from (Keefer et al. 2001). This figure shows the responses of neural cultures on MEAs to various pharmacological agents. Figure B is a close up view of the bottom left of Figure B. Prior experiments with BCC matches results shown above. The effect of antiepilepsy drugs should fall in the bottom left quadrant of B if they effectively attenuate bursting in-vitro.

Differences in bursting duration and interburst interval was used to compare treatment to baseline native activity (Jimbo et al. 2000; Keefer et al. 2001). Standard deviations were calculated for each subject per condition to insure that any differences in the normalized data sets are statistically significant. The change in firing rates and bursting rates during treatment were compared to determine if a relationship to the release kinetics from the monolithic PHEMA drug delivery device can be detected (Ratner 1996). Keefer (Keefer et al. 2001) has previously tested various compounds on a neural culture on a MEA shown in figure 5-4. The results for bicuculline were matched in the PHEMA ring testing. If the antiepilepsy drugs have an effect on bursting like the effect they have on seizures, reduced burst rates and burst durations should appear as points clustered near the origin.

Phase 2: Effect on Stimulated Activity

Phase two of the experiment tested the response to stimulation of a neural culture in the presence of each drug. Response to stimulation was quantified by the average firing rate during a burst. Burst duration and magnitude derived from average firing rates for each drug post stimulation was compared to baseline burst responses. Electrical stimulation of a healthy neural culture produces a stereotypical burst response. Jimbo (Jimbo et al. 2000) describes two phases of a burst, an early phase and a late phase. The early phase is very stereotypical and characterized by synchronous spiking over many channels while spiking seen during the late phase is more random. The metric that Jimbo used to quantify spiking during these phases is the average firing rate. Jimbo varied treatments by increased ion concentrations and showed that the early phase did not change. The late phase changed in response to the same treatments.

Phase 2 consisted of recordings on two dishes with baseline recordings of 20 stimulations thirty seconds apart on a channel with active neurons. This was followed by 20 minutes of probing with stimulations every 30 seconds. The drug was then rinsed and a second baseline was recorded. The next drug was then applied to the culture, probed, and the procedure was repeated for the third and final drug. Spikes were recorded 20ms before each probe and for 800ms afterward. Occasions where spikes occurred before the probe indicate that the probe delivery had occurred during a burst rather than initiating one. Hence, these occasions were excluded from the analysis.

The anti epilepsy drugs should, from researching their effect on the ion channels of the neurons, depress the activity of the culture in general (Hille 1992; Kapur and Macdonald 1997; Brenner 2000). The firing rate for the culture should decrease somewhat and a large increase in interburst interval should be seen. If bursting is epileptiform a very large reduction or complete suppression of bursting should be seen with the proper concentration of drug. The proper concentration could be an issue if high enough concentrations are not reached in the media to even cause an effect. This could be due to problems with the poly HEMA ring as well as problems with the chosen concentration. All concentrations (Brenner 2000; Levy et al. 2002) are 10% of pharmacological blood serum concentrations, which generally corresponds to the concentrations that surround neurons in-vivo due to the blood-brain barrier.

CHAPTER 6
ANTIEPILEPSY DRUG RESULTS AND DISCUSSION

Phase 1 Results

Phenytoin

Figure 6-1 shows interburst interval measured in seconds on the y-axis and the x-axis shows baseline, treatment, and return to baseline results for each MEA. The interburst interval significantly increased for each culture after application of phenytoin relative to baseline measurements. Phenytoin resulted in the eventual complete cessations of bursting over the course of the 20-minute recording, which translates into an infinite interburst interval in each case. This is why each bar is at the ceiling of figure for treatment conditions. Return to baseline results show no difference from baseline measurements suggesting that the washes completely removed phenytoin from the MEA dishes with no apparent carryover effects.

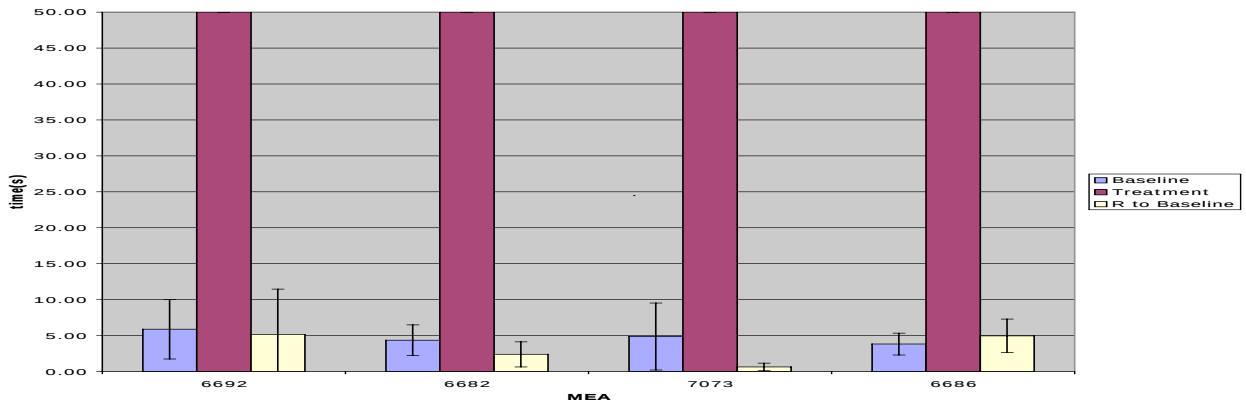

Figure 6-1. Interburst Interval for Phenytoin. Baseline, Treatment, and Return to Baseline results shown for IBI in seconds (on the y-axis) for each of the four dishes (shown on the x-axis) used with phenytoin. Note that IBI approaches infinity as bursting ceased in each dish.

Figure 6-2 shows the burst durations for phenytoin in seconds on the y-axis and baseline, treatment, and return to baseline organized by dish on the x-axis. The quantities of bursts for phenytoin were limited due to the fact that bursting stops about five minutes into the twenty-minute recording for all dishes. Hence the burst durations reported here reflect the culture behavior during these first five minutes rather than the last fifteen minutes where there were no bursts. However, for the bursts that did occur there was little difference from the baseline.

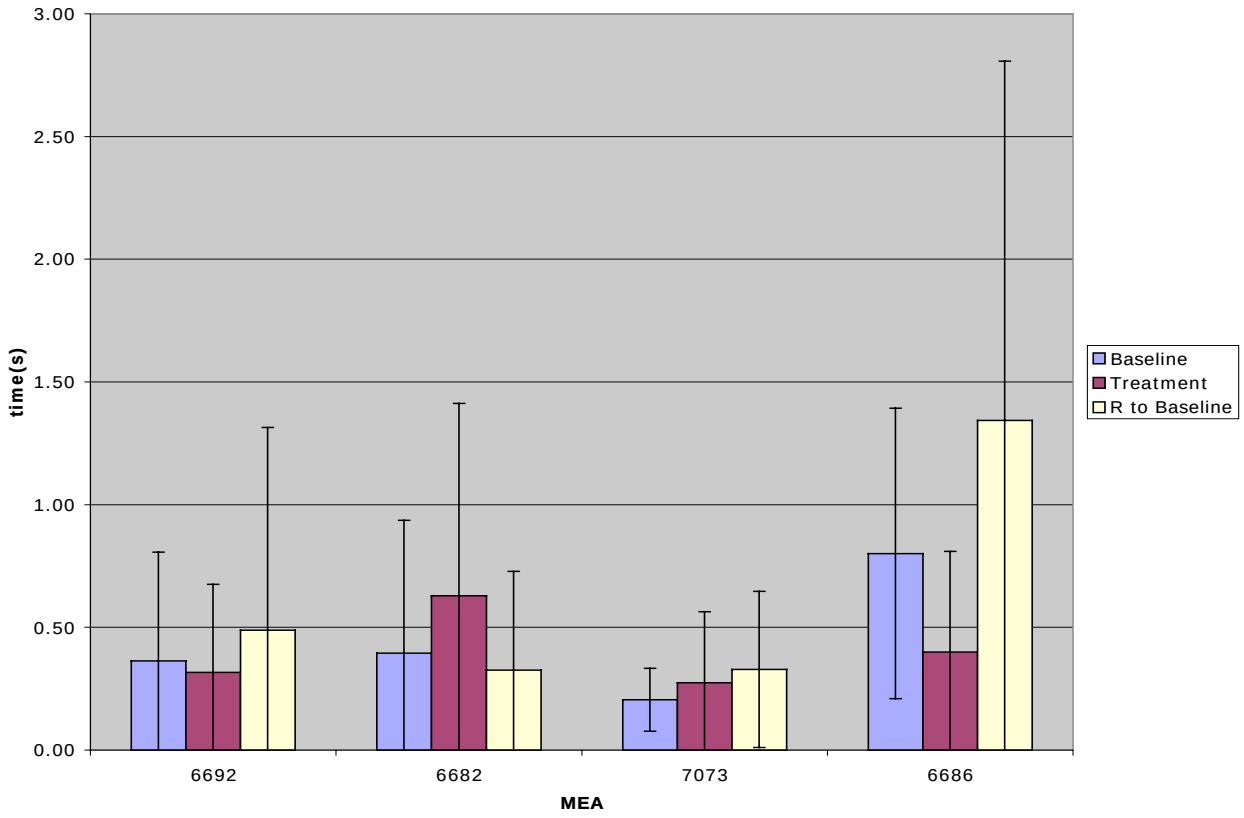

Figure 6-2. Phenytoin Burst Duration. Baseline, Treatment, and Return to Baseline results for BD shown in seconds (on the y-axis) for each of the four dishes (shown on the x-axis) used with phenytoin. Note that no significant difference is seen between baseline, treatment, or return to baseline for all of the dishes.

Figure 6-3 shows an example of raster plots for dish 6686 (one of the four dishes used for phenytoin). The raster plots for the remaining three dishes can be found in Appendix C. Figure 6-3 is made up of four 600-second raster plots The first raster plot represents the baseline recording. The second and third plots represent the first and second half respectively of the continuous treatment run with phenytoin. The fourth plot represents the return to baseline run. Notice the smooth transition in the second plot, beginning at 100s and ending near 400s, between the insertion of the phenytoin laced PHEMA ring at time 0s and the drugged condition as the phenytoin is released from the PHEMA ring.

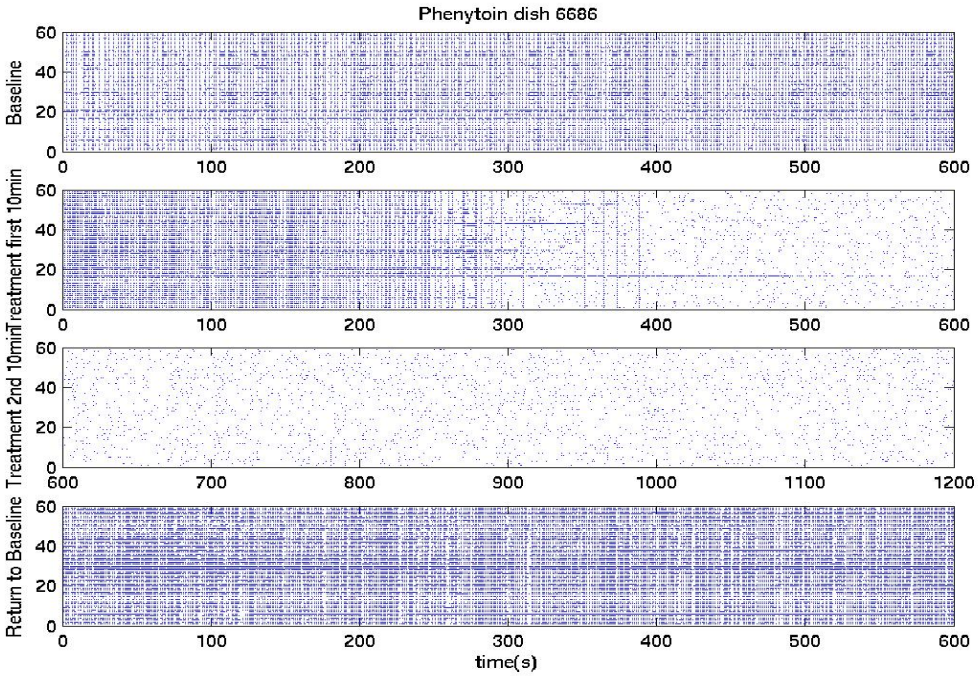

Figure 6-3. Dish 6686 Phenytoin Raster Plots. Each plot has channel number on the y-axis and time on the x-axis. Each point on a given channel at a given time represents an action potential from a nearby neuron. The first raster plot represents the 10-minute baseline recording. The second and third represent the continuous 20-minute treatment recording. The fourth represents the return to baseline recording.

Ethosuximide

Figure 6-4 shows the interburst interval for baseline, treatment, and return to baseline for each culture during application of ethosuximide. This figure shows a difference between baseline and treatment means and their corresponding variances for interburst interval. Only one culture, MEA 7073, resulted in cessations of bursting that translates into an infinite interburst interval. The remaining three cultures show and increased interburst interval that is maintained at a steady state for the remainder of the treatment run. Return to baseline results show no difference from baseline measurements suggesting that the washes completely removed ethosuximide from the MEA dishes with no apparent carryover effects.

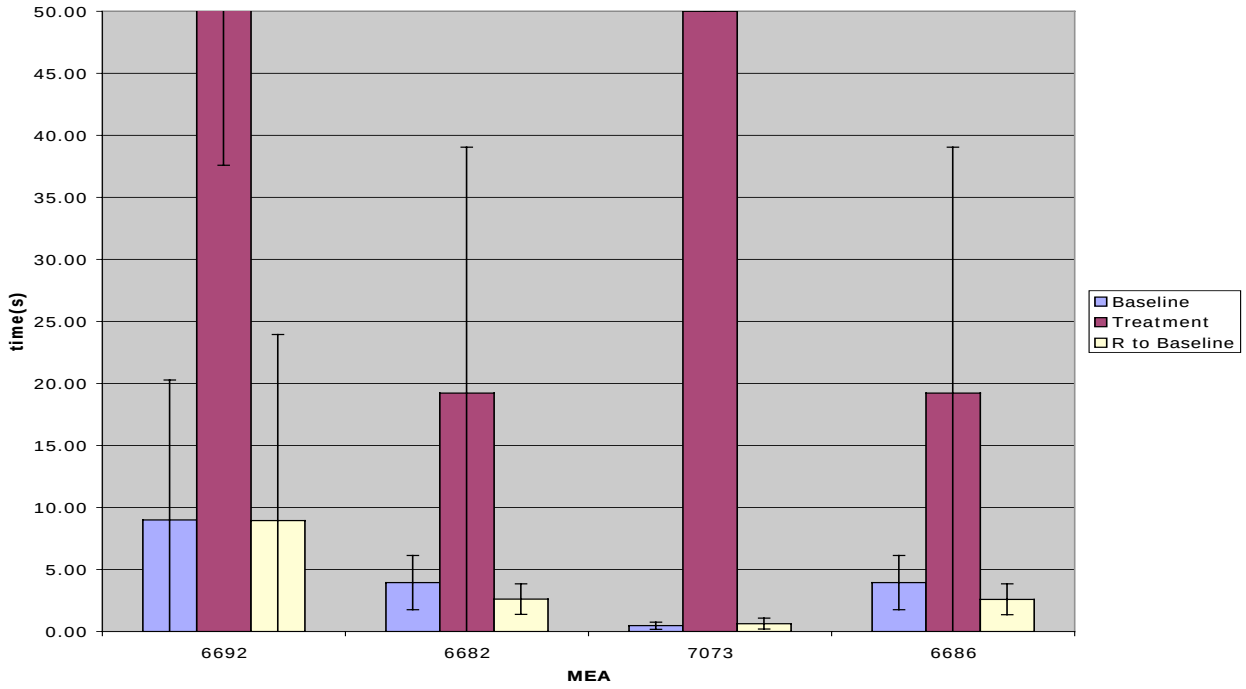

Figure 6-4. Interburst Interval for Ethosuximide. Baseline, Treatment, and Return to Baseline results shown for IBI in seconds (on the y-axis) for each of the four dishes (shown on the x-axis) used with ethosuximide. Note that IBI approaches infinity as bursting ceased in culture 7073 and culture 6692's mean IBI was 128 seconds.

Figure 6-5 shows the burst durations for ethosuximide. There was little difference in burst duration between baseline, treatment, and return to baseline. Even for culture 7073 the burst durations never changed even though bursting ceased completely for this culture.

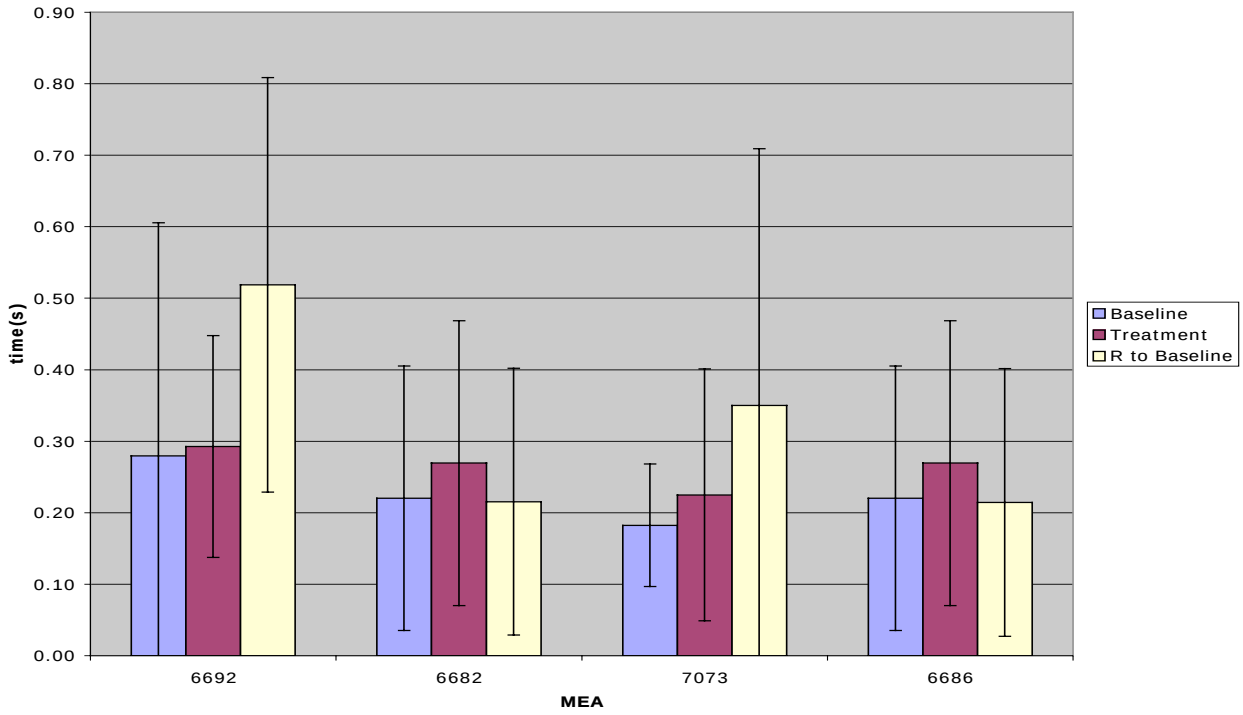

Figure 6-5. Ethosuximide Burst Duration. Baseline, Treatment, and Return to Baseline results for BD shown in seconds (on the y-axis) for each of the four dishes (shown on the x-axis) used with phenytoin. Note that no difference is seen between Baseline, Treatment, or Return to Baseline for all of the dishes.

Figure 6-6 shows the raster plots for dish 6686, one of the four dishes used for ethosuximide. The other three cutures can be found in Appendix D. Figure 6-6 is made up of four 600-second raster plots similar to those for phenytoin. The first raster plot represents the baseline recording. The second and third plots represent the first and second half respectively of the continuous treatment run with ethosuximide. The fourth plot represents the return to baseline run. Application of ethosuximide at 0s eventually

produces an abrupt change in burst activity near 325 seconds relative to native activity and the drugged condition as the ethosuximide is released from the PHEMA ring.

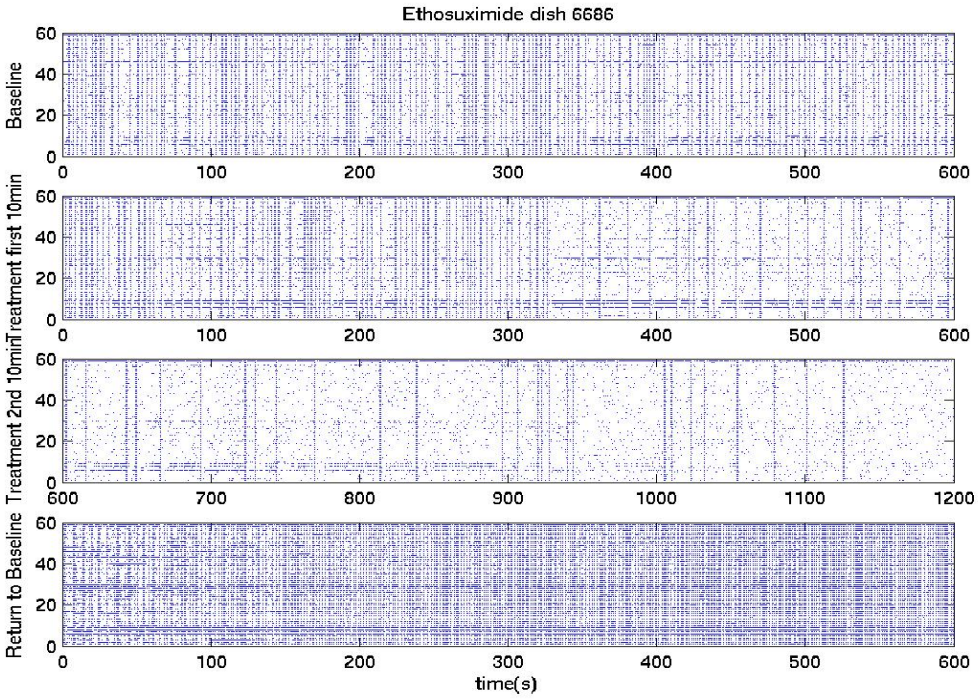

Figure 6-6. Dish 6686 Ethosuximide Raster Plots. Each plot has channel number on the y-axis and time on the x-axis. Each point on a given channel at a given time represents an action potential from a nearby neuron. The first raster plot represents the 10-minute baseline recording. The second and third represent the continuous 20-minute treatment recording. The fourth represents the return to baseline recording.

Valproate

Figure 6-7 shows interburst interval during baseline, treatment, and return to baseline for valproate. This figure shows a large difference between baseline and treatment means and variances for interburst interval. Only one culture, MEA 6692, resulted in cessations of bursting that translates into an infinite interburst interval. The remaining three cultures show an increased interburst interval that is maintained at a steady state for the remainder of the treatment run. Similar to both phenytoin and

ethosuximide there was no difference between baseline and return to baseline and hence, no evidence of carryover effects.

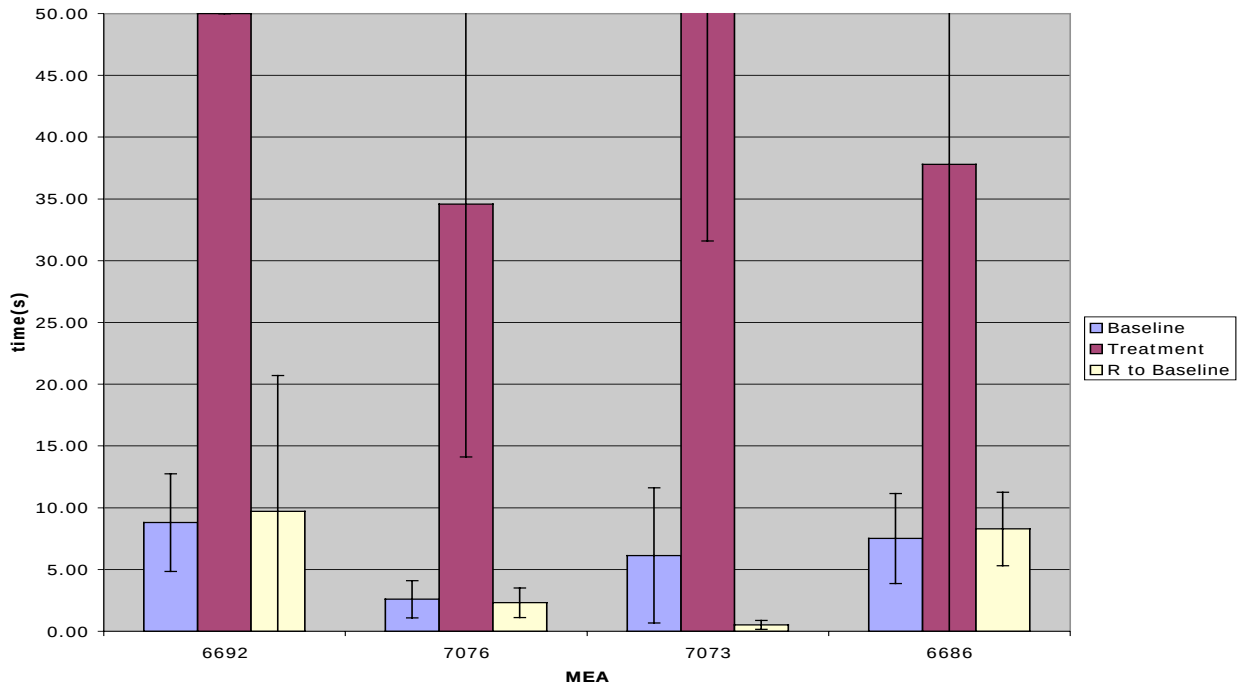

Figure 6-7. Interburst Interval for Valproate. Baseline, Treatment, and Return to Baseline results shown for IBI in seconds (on the y-axis) for each of the four dishes (shown on the x-axis) used with valproate. Note that IBI approaches infinity as bursting ceased in culture 6692 and culture 7073's mean IBI was 120 seconds.

Figure 6-8 shows the correspondent burst durations for valproate. This graph does not show any difference between baseline, treatment, and return to baseline means and variances. There is no significant change in the burst duration when valproate is added to a MEA culture. Even for culture 6692, those bursts that did occur were not different from that of baseline burst durations.

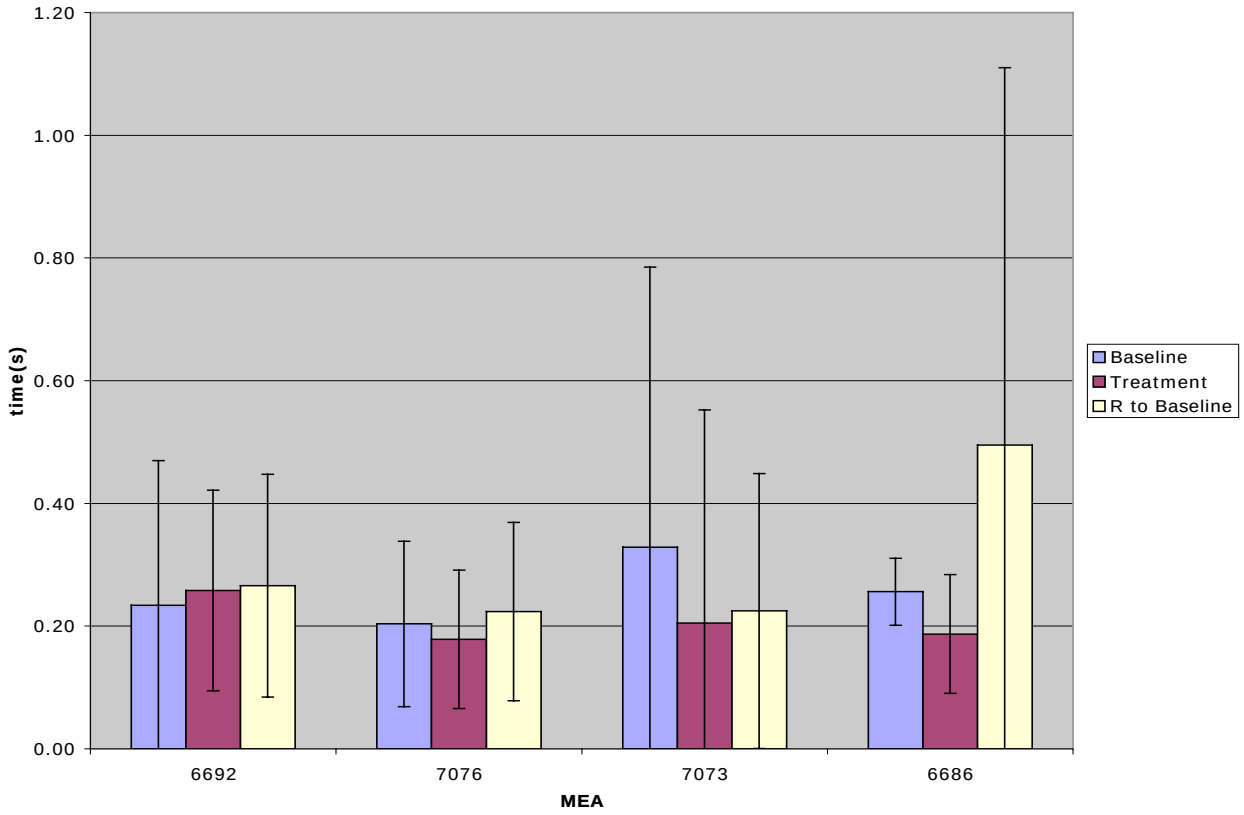

Figure 6-8. Valproate Burst Duration. Baseline, Treatment, and Return to Baseline results for BD shown in seconds (on the y-axis) for each of the four dishes (shown on the x-axis) used with valproate. Note that no difference is seen between Baseline, Treatment, or Return to Baseline for all of the dishes.

Figure 6-9 shows the raster plots for dish 6686 (Appendix E contains the remaining three dishes). Notice the smooth transition between insertion of the PHEMA ring at time zero where activity resembles baseline activity and the drugged condition as the valproate was released from the PHEMA ring.

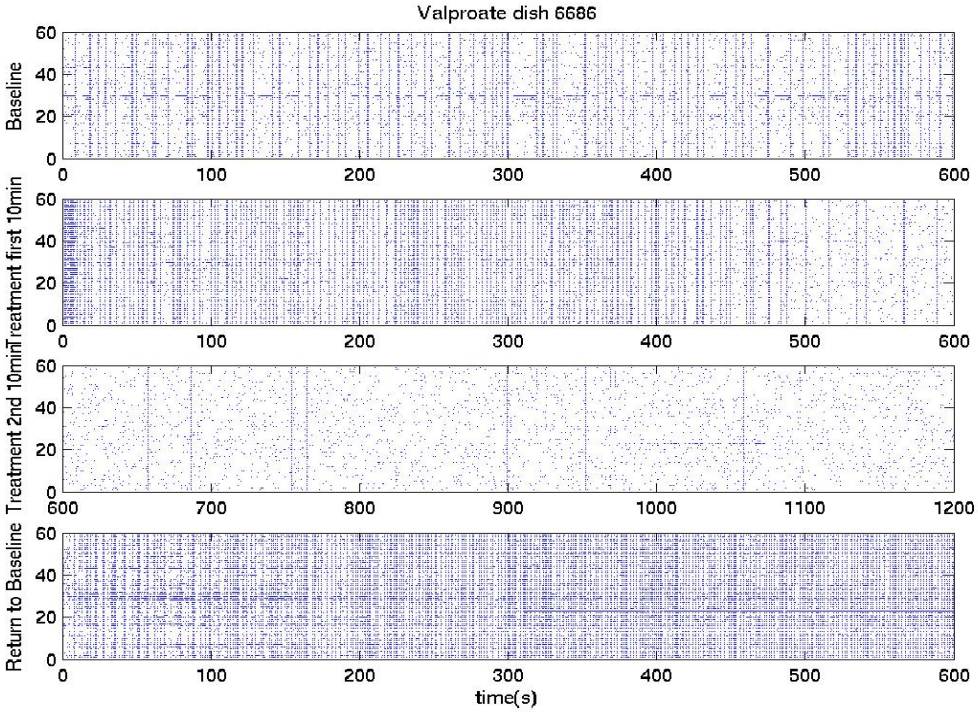

Figure 6-9. Dish 6686 Valproate Raster Plots. Each plot has channel number on the y-axis and time on the x-axis. Each point on a given channel at a given time represents an action potential from a nearby neuron. The first raster plot represents the 10-minute baseline recording. The second and third represent the continuous 20-minute treatment recording. The fourth represents the return to baseline recording.

Summary Phase 1

Each drug resulted in an increase in the interburst interval over time. Phenytoin eventually silenced all bursting in all four dishes resulting in a very large and infinite (bursting ceases) interburst interval that translates to a zero bursting rate. Valproate and ethosuximide slowed the bursting rates of three of four dishes in each case while silencing the fourth dish. Burst duration was not effected by any of the three drugs. The mean burst duration moved very little in any dish with any drug and the standard deviations of the data heavily overlapped suggesting that there is no distinguishable difference in the burst duration between baseline and drugged states.

Phase 2 Results

Stimulation of drugged dishes paralleled the results of Phase 1 in that phenytoin had the largest effect on the cultures. Valproate and ethosuximide did little to prevent bursting after an electrical stimulation. Figures 6-10 and 6-11 show that phenytoin treatments reduce or eliminate the burst response to stimulation seen in baseline recordings in-vitro.

The 20 stimulations events for each condition were recorded into a single file for each condition. Each stimulation event starts with a 500mV 200us biphasic pulse. The average firing rate for each run is determined by creating a histogram of all spikes following the stimulation. The spikes that make up the resulting burst are sorted into 1ms bins. The algorithm that does this sorting is shown in Appendix A. The resulting bins are graphed in chronological order to show the average firing rate of the resulting burst post-stimulation.

Figure 6-10 shows the response to stimulation for dish 6686. Phenytoin, shown in the second graph had a noticeable effect on the average firing rate of the culture during the initial early phase where a small number of action potentials can be seen. Phenytoin almost completely eliminates the late phase bursting response. Both valproate and ethosuximide show a small but consistent increase in average firing rate compared to the baseline conditions over the first 30ms for this culture.

Figure 6-11 shows the response to stimulation for dish 1534. This was the first time drugs were applied to this dish. The early phase for each drug and all baselines were nearly identical. Valproate and phenytoin both show little deviation from the baseline conditions in the late phase. The results are similar to dish 6686 in that only phenytoin

has a large noticeable effect on response to stimulation. However, dish 1534s average firing rate for phenytoin during the late phase was only reduced not eliminated.

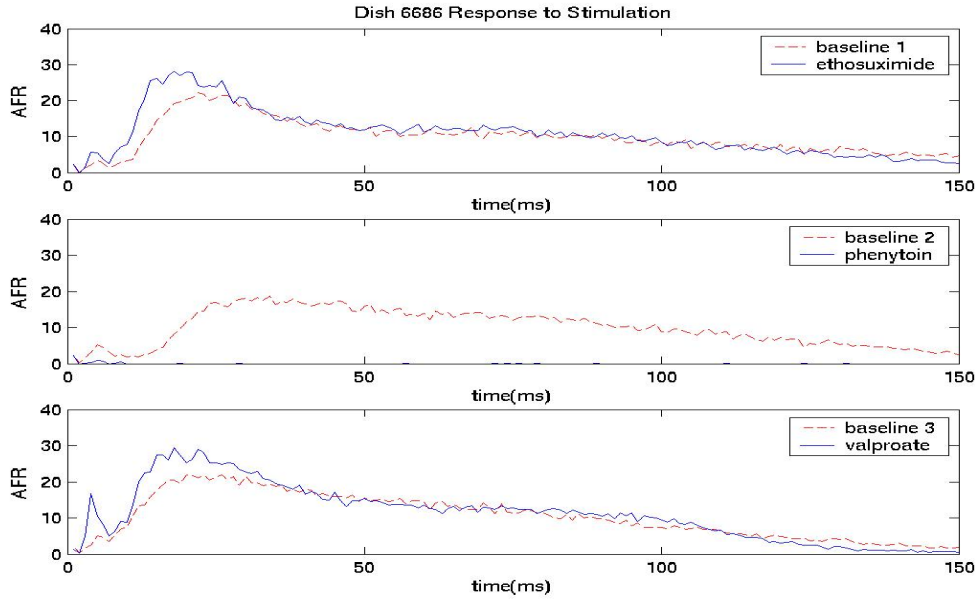

Figure 6-10. Dish 6686 Response to stimulation. The y-axis of this figure is a count of the average number of action potentials detected for each time bin over the 20 stimulation events.

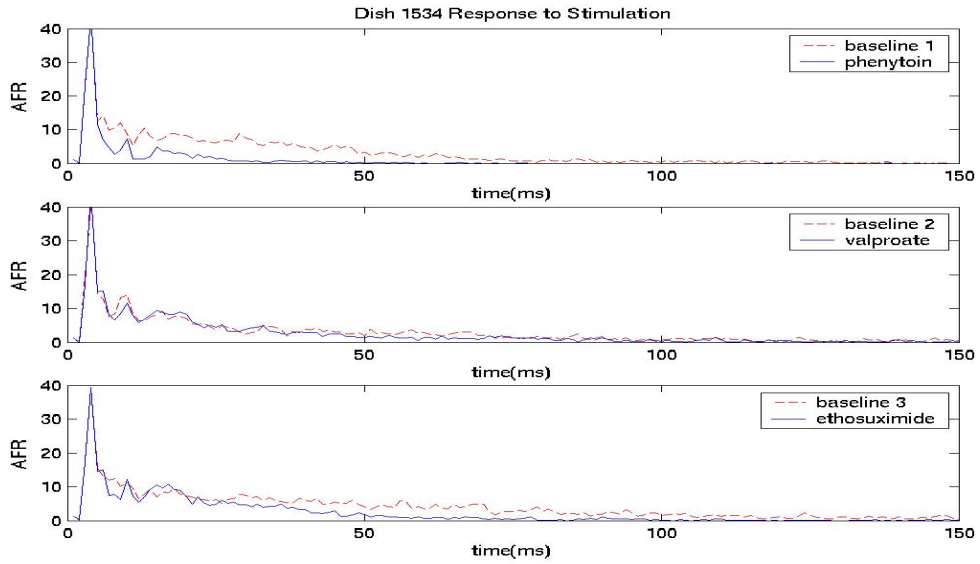

Figure 6-11. Dish 1534 Response to stimulation. The y-axis of this figure is a count of the average number of action potentials detected for each time. This graph shows the average shape of a burst from 20 stimulation events.

The first 15ms after stimulation differ greatly for the two dishes. They both show large spikes synchronized activity within the first 5ms. It is possible that some of this initial activity is artifact from the stimulation. A dish-to-dish comparison shows enormous differences during the early phase. Only phenytoin indicates any major differences between baseline and treatment for dish 1534. After the initial 6-10ms phenytoin demonstrates less than 40% of the activity of the baseline conditions. Dish 6686 shows differences in each case between baseline and treatment conditions. For phenytoin there are fewer action potentials and only a few channels in close proximity to the stimulating electrode that show and signs of action potentials. When drugs are present for both valproate and ethosuximide the early phase demonstrates more action potentials.

Discussion and Conclusions

Discussion

If in-vitro bursting is similar to in-vivo epilepsy antiepilepsy the drugs used for treating in-vivo epilepsy should have similar effects on in-vitro bursting. When a properly diagnosed patient takes phenytoin for grand mal (tonic-clonic) epilepsy the patient can expect to have a reduction in grand mal seizure activity (Levy et al. 2002). Phenytoin also increases the voltage threshold for seizures caused by electrical stimulation in animals and humans (electroshock therapy). Phenytoin has been shown to be ineffective in the treatment of petit mal (absence) seizures. Phenytoin silences in-vitro bursting within the first 6-7 minutes in these experiments and the response to stimulation for phenytoin was similar to in-vivo. That is, bursting in response to stimulation is either largely reduced or eliminated with phenytoin. The main mechanism of action for phenytoin is the blockage of voltage sensitive sodium channels that are important for initiating action potentials. When these channels are blocked the likelihood of a neuron

responding to electrical stimulation from electrodes or a nearby neuron is reduced (Hille 1992). It is logical that blockage of these channels would reduce epileptic seizures and bursting in-vitro.

Ethosuximide is a successful drug for the treatment of absence seizures but fairly ineffective in the prevention of grand mal seizures (Levy et al. 2002). Similarly the experiment in-vitro indicates ethosuximide is the least effective of the three drugs tested in terms of its ability to stop or slow the bursting. It does cause what appears to be a sudden change in the burst rate for all treatment runs. This phase change results in a slowed bursting rate but does not lead to a cessation of burst behavior. Ethosuximide does little to nothing to prevent bursts in response to electrical stimulation in-vitro. The application of ethosuximide may have actually increased the average firing rate of neurons in the early phase of bursting in one dish. Its mechanisms of action, which are poorly understood, do little to make it effective as an anticonvulsant in-vivo. In-vitro it is not able to eliminate bursting or prevent bursting in response to stimulation.

Valproate is a drug with many actions within the nervous system that make it an effective antiepilepsy drug for both grand mal and petit mal seizures(Levy et al. 2002). In-vitro valproate shows similarities to phenytoin in that a smooth change in bursting rate occurs over a long period of time. The data seems to indicate the steady state may not have been reached in the experimental window for treatment conditions. It is possible that longer exposure to valproate may cause bursting to cease in-vitro. However, valproate is similar to ethosuximide in that it did not fully stop bursting in most dishes and also did little to prevent bursting responses from electric stimulation. As one might

expect the results for valproate are mixed as exactly how valproate works to prevent many forms of seizures are not fully understood.

Conclusions

Overall the experiments suggest that phenytoin was the most effective drug in the prevention of bursting by neural cultures. Valproate was the next most effective drug with ethosuximide having the least effect on the cessation of bursting. All three drugs increased the interburst interval resulting in a slowed the bursting rate, and phenytoin completely eliminates bursting. However, none of the drugs had an effect on burst duration.

It stands to reason that if in-vivo epilepsy and in-vitro bursting share common behaviors that treatment of bursting with antiepilepsy drugs should determine whether they might share similar origins. In-vitro bursting does indeed show a similar response to antiepileptic drugs as in-vivo epileptic seizures. It also stands to reason that the cultures may respond better to drugs meant for a specific type of epilepsy. In fact this experiment shows that in-vitro bursting responds better to one type of epilepsy treatment than others. The effects of phenytoin on the neural cultures bursting behavior suggest that in-vitro bursting may be most similar to in-vivo grand mal (tonic-clonic) seizures. However, since the drugs tested only treat symptoms of seizures it is still possible that the causes of seizure in-vitro and in-vivo may be very different.

This evidence does suggest that further investigation is warranted. The presence of these effects is important not only for its relevance to similarities between the in-vivo and in-vitro systems, but it would also open the possibility of the study of epilepsy in an in-vitro system that permits detailed (multi-channel) long term recordings on a platform where experimental manipulation is more easily accomplished.

APPENDIX A
BURST DETECTION ALGORITM

Burstdet.m – this is the main burst detection function it only requires data in the form of a spikefile from MEABench.

```
function [bst,burstdata,globalrate] = burstdet(data)
time = 0.00004;
leaky = zeros(3,60);
burst = 0;


A = data.time;
B = data.channel;
N = length(A);
J = 1;
globalrate = A * 0;
burstdata = A * 0;
decay = 0.9999;

for I = 1:N
   if B(I) <= 59
      %if A(I) >= 180

      dtime = A(I) - leaky(1,(B(I)+1));
      lastspike = max(leaky(1,(B(I)+1)));
      leaky(2,:) = leaky(2,:) * (decay^(25000* (dtime)));
      leaky(2,(B(I)+1)) = leaky(2,(B(I)+1)) + 1;
      globalrate(I) = sum(leaky(2,:))/60;
      leaky(1,(B(I)+1)) = A(I);
      %end
   end
end
C= median(globalrate(1:I));
D = std(globalrate(1:I));
threshold = C + 0.25*D; %0.25

for I = 1:N
   if B(I) <= 59
      %if A(I) >= 180
```

```
   dtime = A(I) - leaky(1,(B(I)+1));

   leaky(2,(B(I)+1)) = leaky(2,(B(I)+1)) * (decay^(25000* (dtime))) + 1;
   %globalrate(I) = sum(leaky(2,:))/60;

   if burst == 1
      lastspike = max(leaky(1,(B(I)+1)));
      Z = I-1;
      if (A(I) - A(Z)) >= 0.05 %0.05
         if (A(Z) - bst(J,1)) >= 0.10
            burst = 0;
            burstdata(I-1) = 0;
            bst(J,2) = A(Z);
            bst(J,3) = bst(J,2) - bst(J,1);
            J = J + 1;
         end
      end
   end
   if burst == 0
      %if A(I) >= 180
         if globalrate(I) > threshold
            burst = 1;
            bst(J,1) = A(I);
         end
         %end
   end
   burstdata(I)=burst;
   leaky(1,(B(I)+1)) = A(I);
   %end
   end
end
figure
subplot(3,1,1);plot(data.time,burstdata); axis([1 600 0 1.5]);
subplot(3,1,2);plot(data.time,globalrate); axis([1 600 0 2]);
subplot(3,1,3);plot(data.time,data.channel,'.','markersize',1);axis([1 600 0 60]);
```

burstrate.m – this file calls the burstdet function to create files with burst data and also creates files with statistical data on the bursts.

```
function [rundata,runstats] = burstdet(data1,data2,data3)

[bursts1,burstdata1,globalrate1] = burstdet(data1);
[bursts2,burstdata2,globalrate2] = burstdet(data2);
[bursts3,burstdata3,globalrate3] = burstdet(data3);
```

```
rundata =
struct('bursts1',[bursts1],'burstdata1',[burstdata1],'globalrate1',[globalrate1],'bursts2',[burs
ts2],'burstdata2',[burstdata2],'globalrate2',[globalrate2],'bursts3',[bursts3],'burstdata3',[bur
stdata3],'globalrate3',[globalrate3]);
runstats = struct('rates',[length(bursts1) length(bursts2)
length(bursts3)],'meanburstduration',[mean(bursts1(:,3)) mean(bursts2(:,3))
mean(bursts3(:,3))],'stdburstduration',[std(bursts1(:,3)) std(bursts2(:,3)) std(bursts3(:,3))])
```

burst.m – this file ties everthing together when three sets of data (baseline, treatment, return to baseline are used.

```
[rundata,runstats] = burstrate(data1,data2,data3)
```

APPENDIX B
RASTER PLOTS FOR BICUCULLINE TREATMENTS

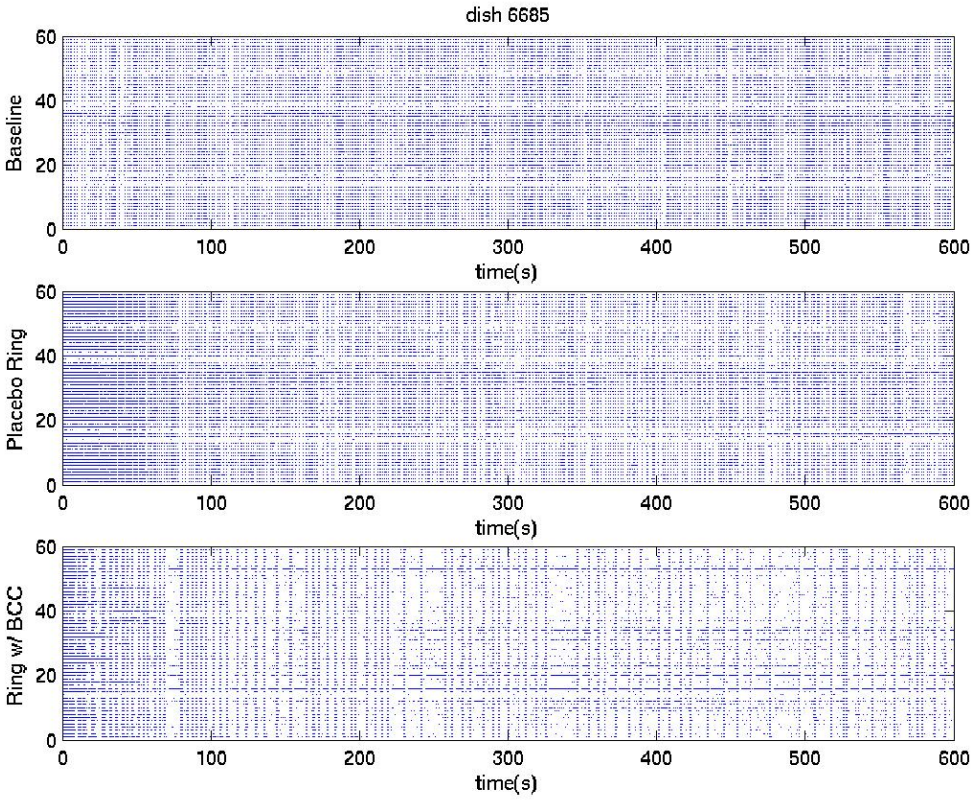

Figure B-1. Raster plots of spike activity for dish 6685 during baseline, placebo, and bicuculline treatment spike activity. Time is on the x-axis in seconds and channel in hardware order is on the y-axis each point represents an action potential from a nearby neuron.

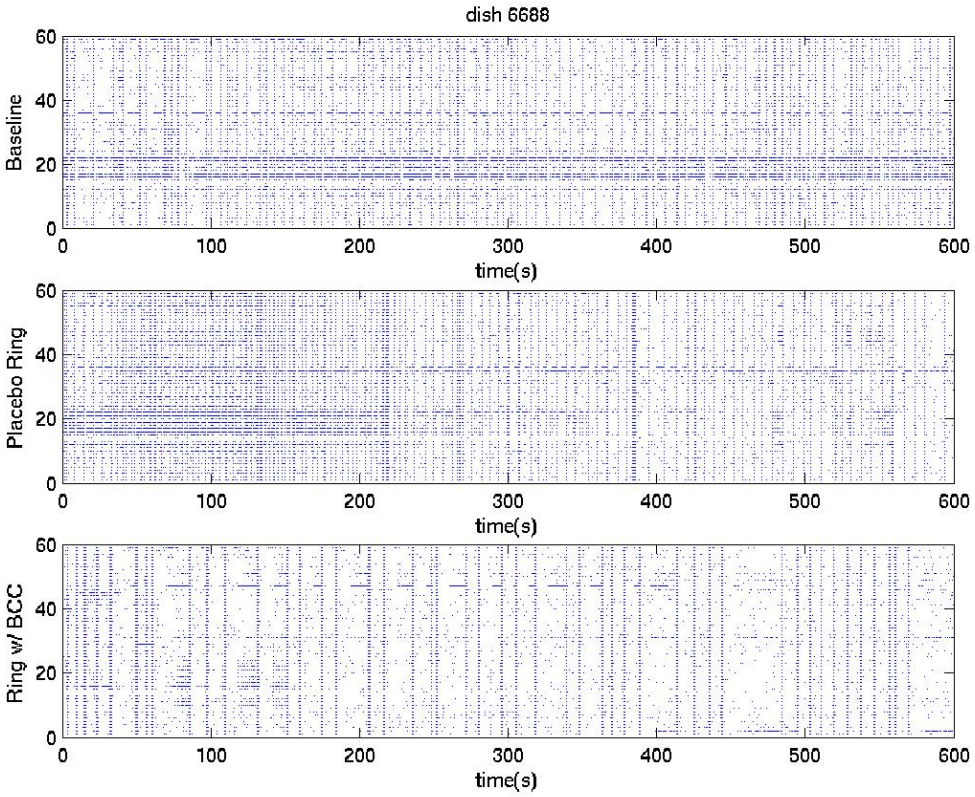

Figure B-2. Raster plots of spike activity for dish 6688 during baseline, placebo, and bicuculline treatment spike activity. Time is on the x-axis in seconds and channel in hardware order is on the y-axis each point represents an action potential from a nearby neuron.

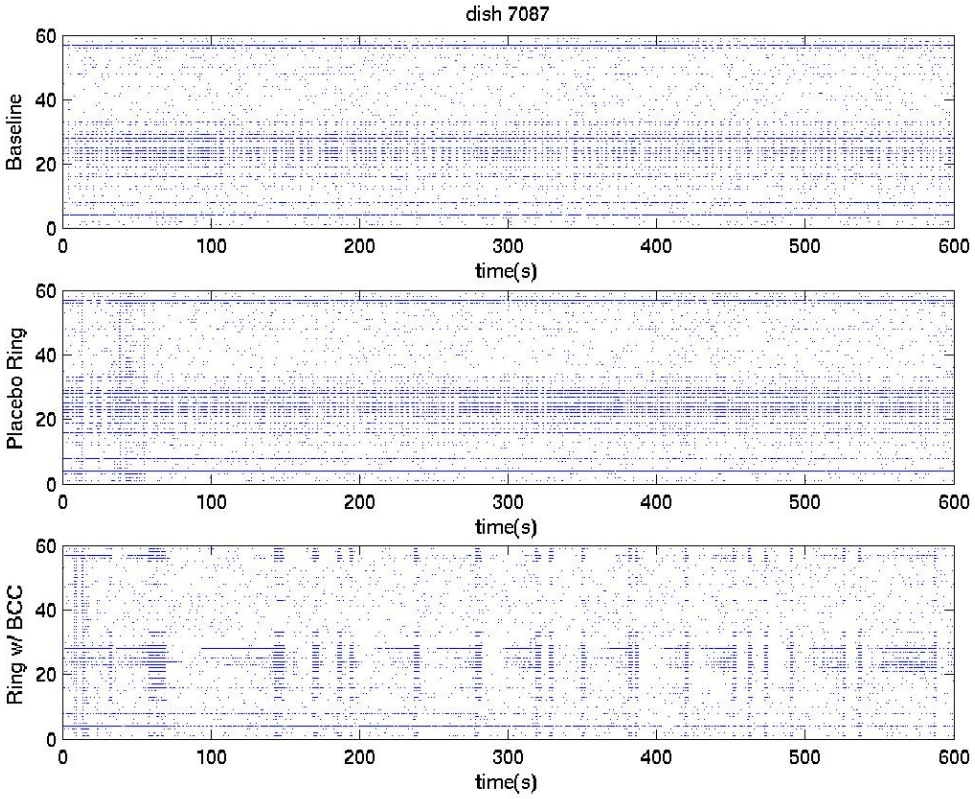

Figure B-3. Raster plots of spike activity for dish 7087 during baseline, placebo, and bicuculline treatment spike activity. Time is on the x-axis in seconds and channel in hardware order is on the y-axis each point represents an action potential from a nearby neuron.

APPENDIX C
RASTER PLOTS FOR PHENYTOIN

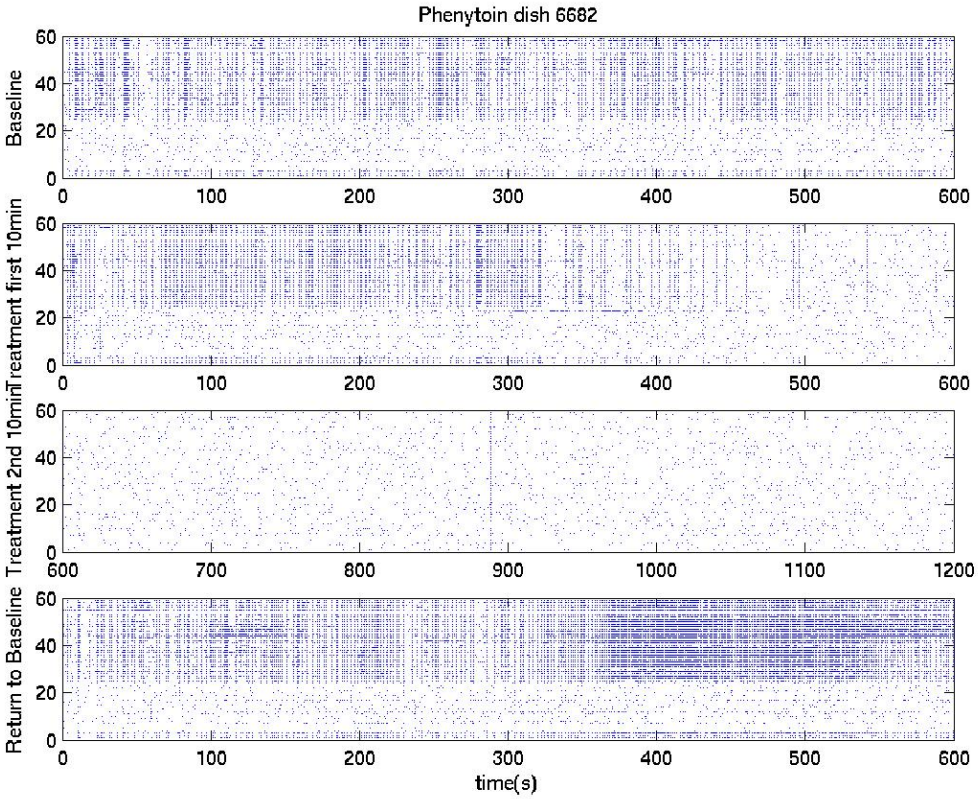

Figure C-1. Dish 6682 Phenytoin Raster Plots. Each plot has channel number on the y-axis and time on the x-axis. Each point on a given channel at a given time represents an action potential from a nearby neuron. The first raster plot represents the 10-minute baseline recording. The second and third represent the continuous 20-minute treatment recording. The fourth represents the return to baseline recording.

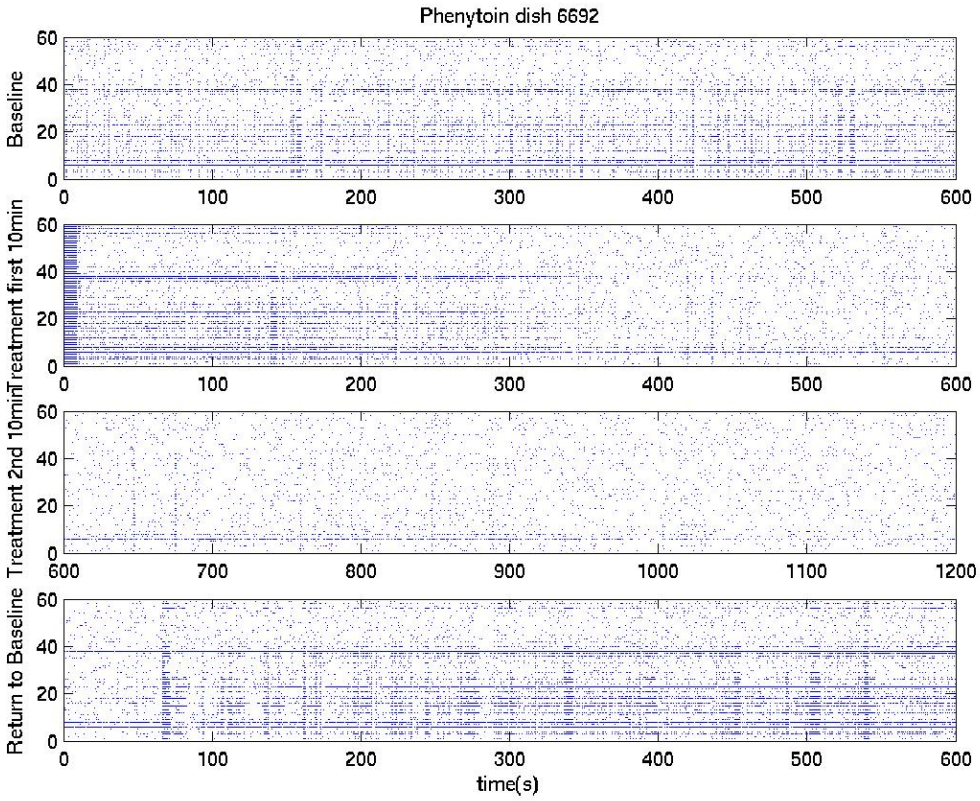

Figure C-2. Dish 6692 Phenytoin Raster Plots. Each plot has channel number on the y-axis and time on the x-axis. Each point on a given channel at a given time represents an action potential from a nearby neuron. The first raster plot represents the 10-minute baseline recording. The second and third represent the continuous 20-minute treatment recording. The fourth represents the return to baseline recording

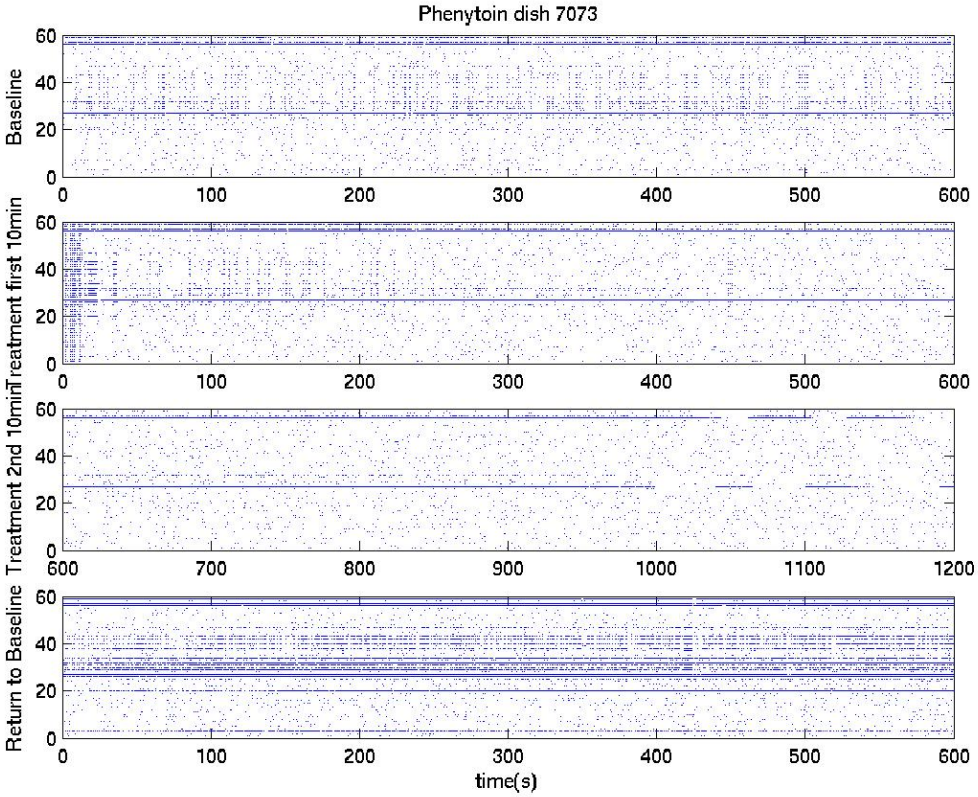

Figure C-3. Dish 7073 Phenytoin Raster Plots. Each plot has channel number on the y-axis and time on the x-axis. Each point on a given channel at a given time represents an action potential from a nearby neuron. The first raster plot represents the 10-minute baseline recording. The second and third represent the continuous 20-minute treatment recording. The fourth represents the return to baseline recording

APPENDIX D
RASTER PLOTS FOR ETHOSUXIMDE

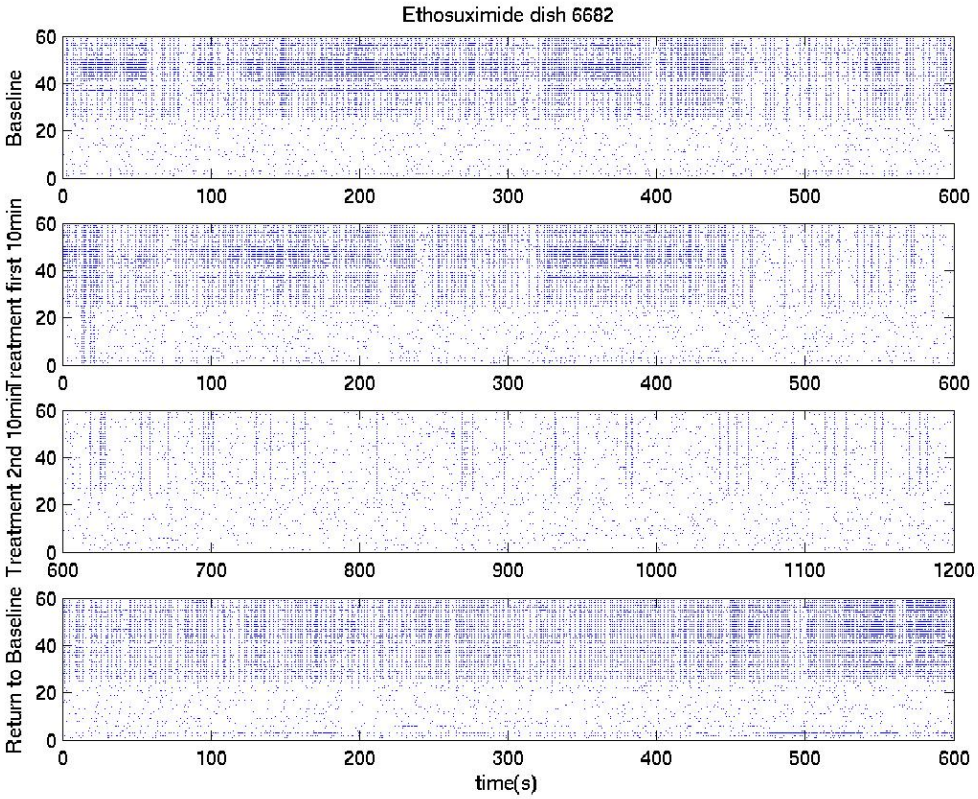

Figure D-1. Dish 6682 ethosuximide Raster Plots. Each plot has channel number on the y-axis and time on the x-axis. Each point on a given channel at a given time represents an action potential from a nearby neuron. The first raster plot represents the 10-minute baseline recording. The second and third represent the continuous 20-minute treatment recording. The fourth represents the return to baseline recording

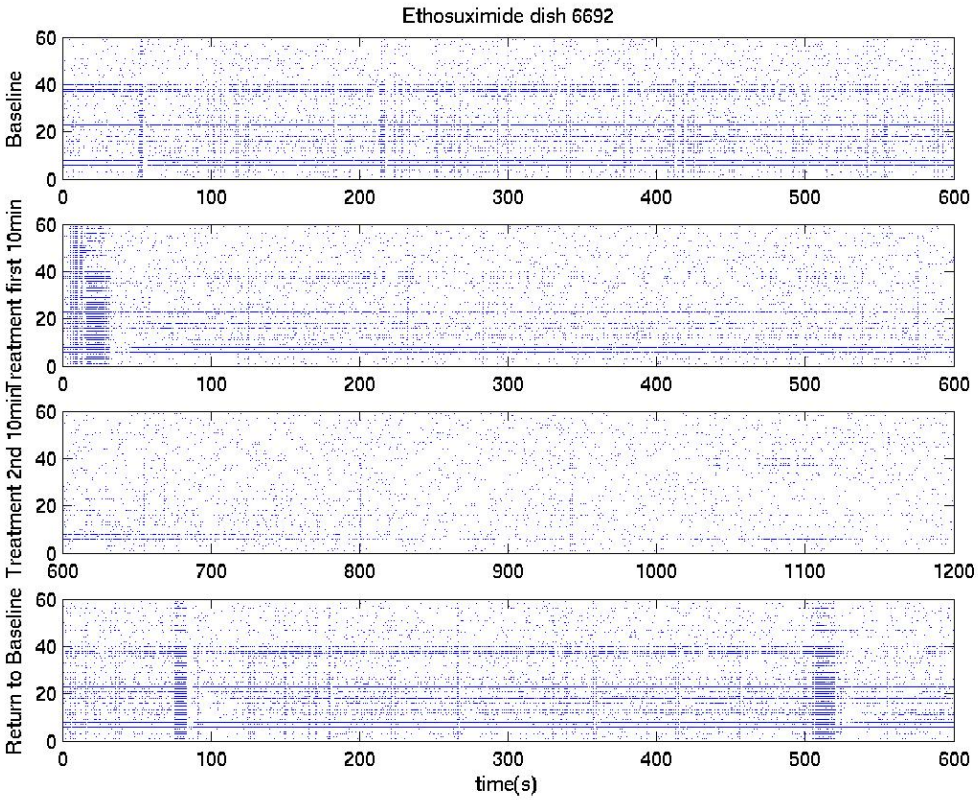

Figure D-2. Dish 6692 ethosuximide Raster Plots. Each plot has channel number on the y-axis and time on the x-axis. Each point on a given channel at a given time represents an action potential from a nearby neuron. The first raster plot represents the 10-minute baseline recording. The second and third represent the continuous 20-minute treatment recording. The fourth represents the return to baseline recording

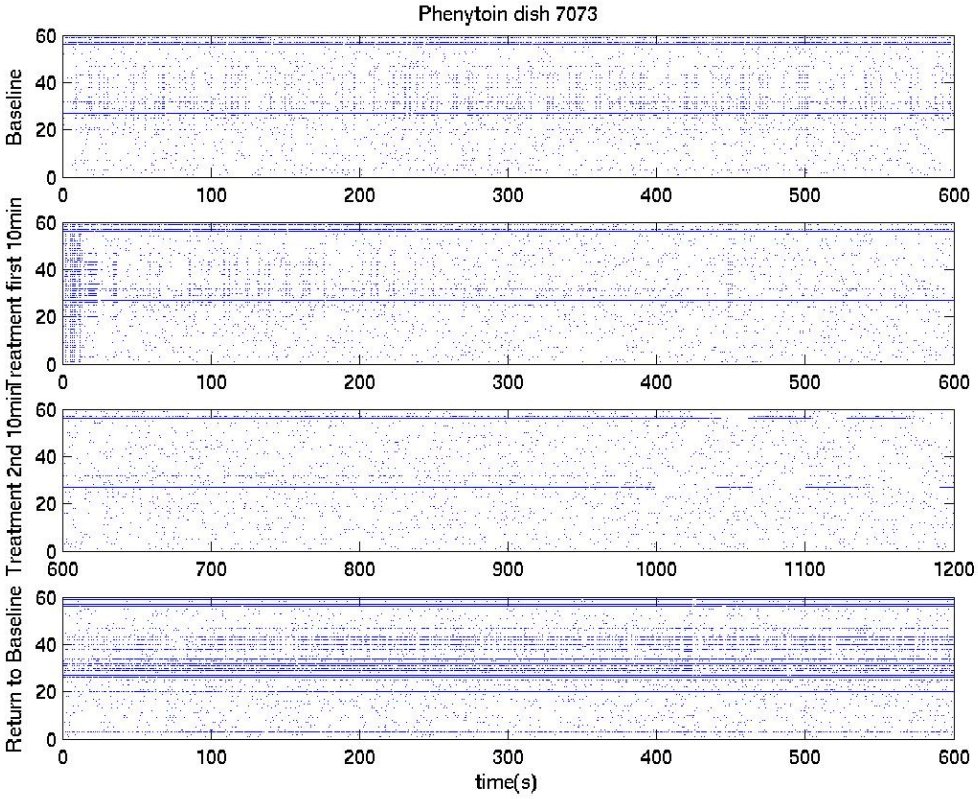

Figure D-3. Dish 7073 ethosuximide Raster Plots. Each plot has channel number on the y-axis and time on the x-axis. Each point on a given channel at a given time represents an action potential from a nearby neuron. The first raster plot represents the 10-minute baseline recording. The second and third represent the continuous 20-minute treatment recording. The fourth represents the return to baseline recording

APPENDIX E
RASTER PLOTS FOR VALPROATE

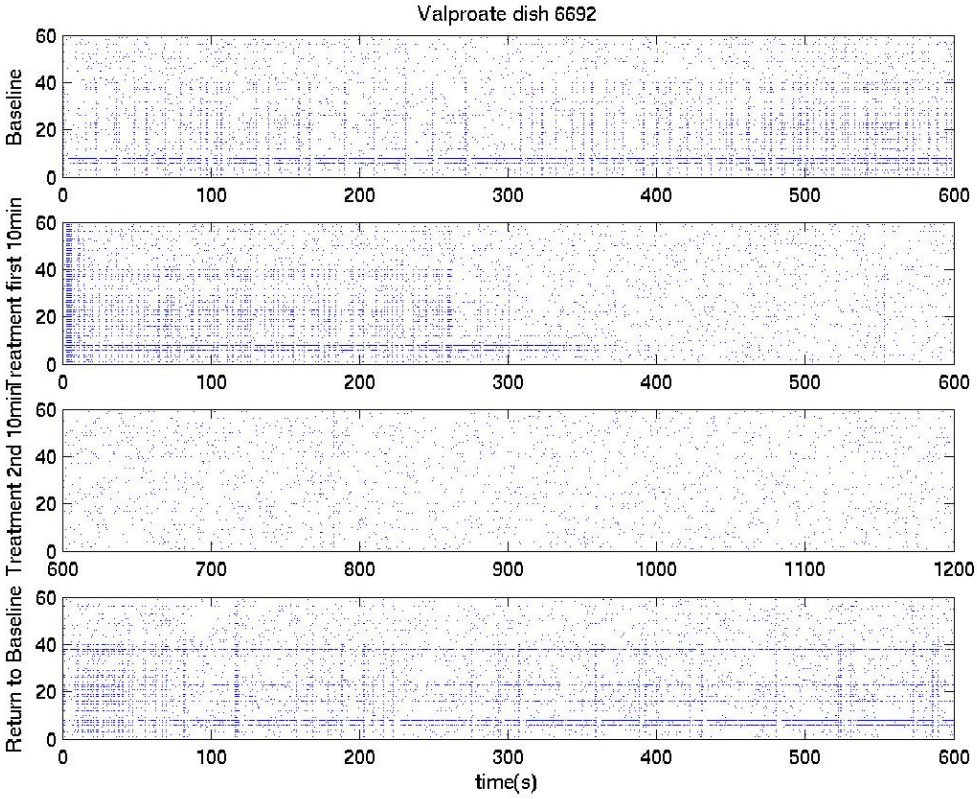

Figure E-1. Dish 6692 valproate Raster Plots. Each plot has channel number on the y-axis and time on the x-axis. Each point on a given channel at a given time represents an action potential from a nearby neuron. The first raster plot represents the 10-minute baseline recording. The second and third represent the continuous 20-minute treatment recording. The fourth represents the return to baseline recording

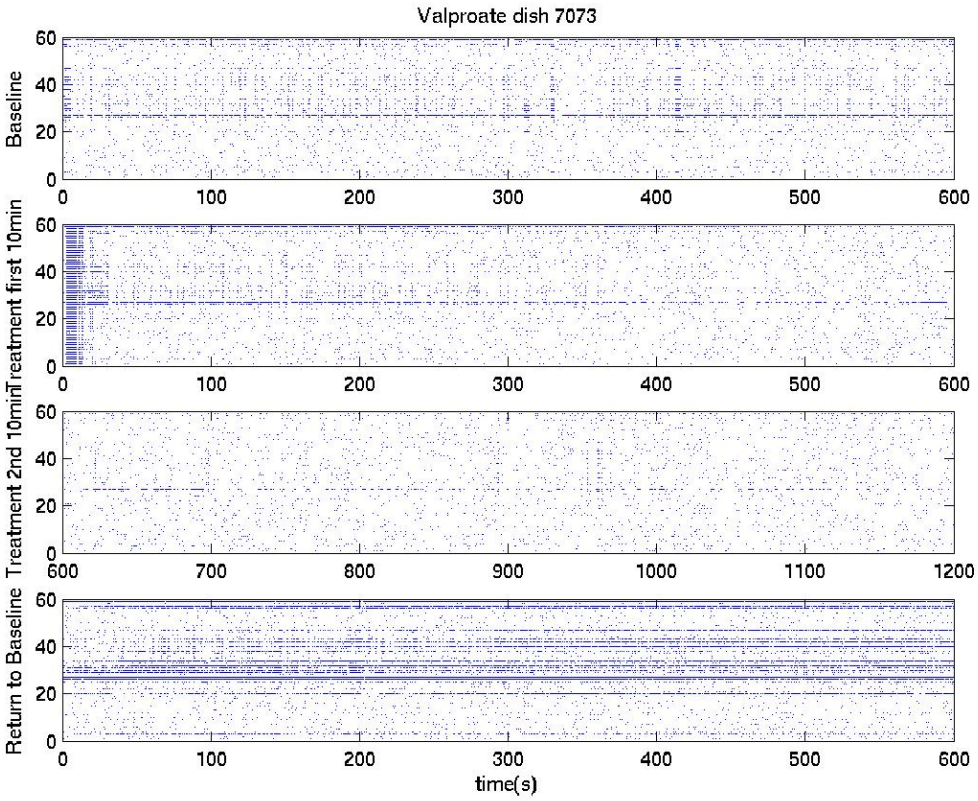

Figure E-2. Dish 7073 valproate Raster Plots. Each plot has channel number on the y-axis and time on the x-axis. Each point on a given channel at a given time represents an action potential from a nearby neuron. The first raster plot represents the 10-minute baseline recording. The second and third represent the continuous 20-minute treatment recording. The fourth represents the return to baseline recording

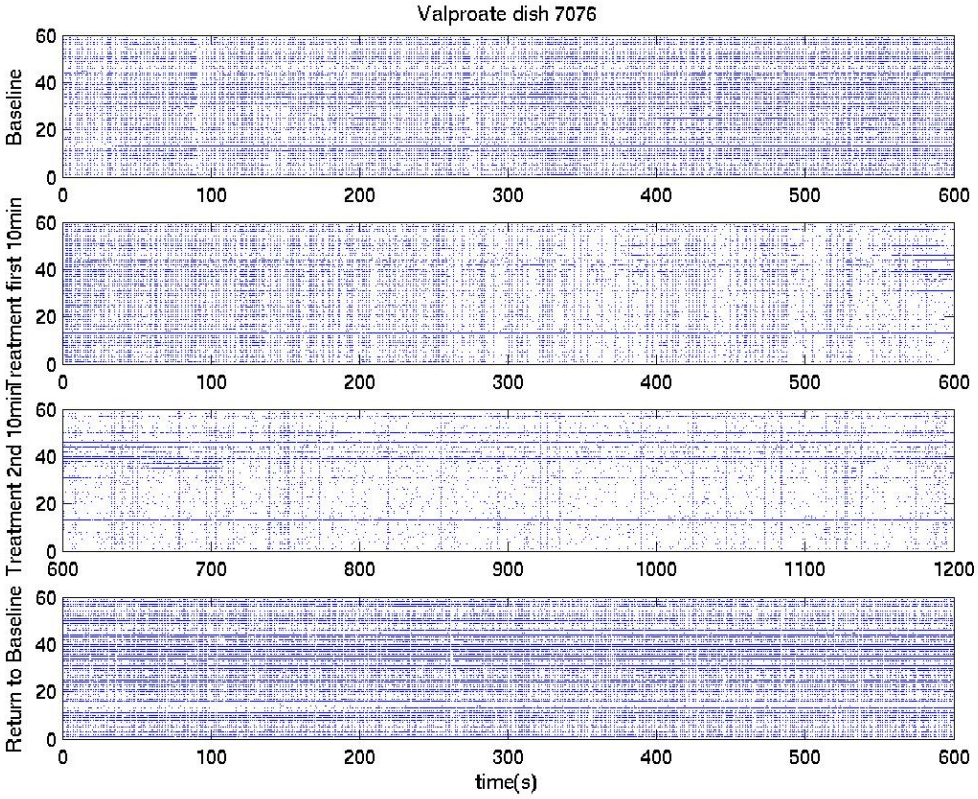

Figure E-3. Dish 7076 valproate Raster Plots. Each plot has channel number on the y-axis and time on the x-axis. Each point on a given channel at a given time represents an action potential from a nearby neuron. The first raster plot represents the 10-minute baseline recording. The second and third represent the continuous 20-minute treatment recording. The fourth represents the return to baseline recording

LIST OF REFERENCES

Banker, Goslin (1998) Culturing Nerve Cells. MIT Press: Cambridge, Massachusetts.

Bledi Y, Domb AJ, Linial M (2000) Culturing Neuronal Cells on Surfaces Coated by a Novel Polyethyleneimine-Based Polymer. Brain Research Protocols 5:282-289.

Brenner GM (2000) Pharmacology. WB Saunders Company: Philadelphia, PA.

Bugard EC, Hablitz JJ (1993) Developmental Changes in NMDA and Non-NMDA Receptor-Mediated Synaptic Potentials in Rat Neocortex. Journal of Neurophysiology 69:230-240.

Claverol-Tinture E, Pine J (2002) Extracellular Potentials in Low-density Dissociated Neuronal Culture. Journal of Neuroscience Methods 117:13-21.

DeLorenzo RJ, Pal S, Sombati S (1998) Prolonged Activation of the N-methyl-D-aspartate Receptor – Ca2+ Transduction Pathway Causes Spontaneous Recurrent Epileptiform Discharges in Hippocampal Neurons in Culture. Proceedings of the National Academy of Science USA 95:14482-14487.

DeMarse TB, Wagenaar DA, Blau AW, Potter SM (2001) The Neurally Controlled Animat: Biological Brains Acting with Simulated Bodies. Autonomous Robots 11:305-310.

Egert U, Hammerle H (2002) Application of the Microelectrode-Array (MEA) Technology in Pharmaceutical Drug Research. Baselt JP and Gerlach G (editors) Sensoren im Fokus neuer Anwendugen Web Univeritatsverlag, Dresden:51-54.

Egert U, Heck D, Aertsen A (2002) Two-dimensional Monitoring of Spiking Networks in Acute Brain Slices. Experimental Brain Research 142:268-274.

Egert U, Schlosshauer B, Fennrich S, Nisch W, Fejtl M, Knott T, Muller T, Hammerle H (1998) A Novel Organotypic Long-term Culture of the Rat Hippocampus on Substrate-integrated Multielectrode Arrays. Brain Research Protocols 2:229-242.

Freeman WJ (1994) Neural Networks and Chaos. Journal of Theoretical Biology 171:13-18.

Garcia PS, Calabrese RL, DeWeerth SP, Ditto WL (2002) Simple Arithmetic with Firing Rate Encoding in Leech Neurons: Simulation and Experiment (Pre-print).

Available on the WWW at
http://wwwneuroengineeringcom/publications/111180pdf. 7/6/04

Gluckman BJ, Neel EJ, Netoff TI, Ditto WL, Spano ML, Schiff SJ (1996) Electric Field Suppression of Epileptiform Activity in Hippocampal Slices. Journal of Neurophysiology 96:4202-4205.

Goldberg ea (2002) Polymeric Biomaterials EMA 6581 Laboratory Handout, Fall 2002. Department of Materials Science and Engineering, University of Florida.

Gross GW, Kowalski JM (1999) Origins of Activity Patterns in Self-Organizing Neuronal Networks in Vitro. Journal of Intelligent Material Systems and Structures 10:558-564.

Gross GW, Rieske E, Kreutzberg GW, Meyer A (1977) A New Fixed-array Multielectrode System Designed for Long-term Monitoring of Extracellular Single Unit Neuronal Activity In-vitro. Neuroscience Letters 6:101-105.

Guehl D, Burbaud P, Boraud T, Bioulac B (2000) Bicuculline Injections into the Rastral and Caudal Motor Thalamus of the Monkey Induce Different Types of Dystonia. European Journal of Neuroscience 12:1033-1037.

Hille B (1992) Ionic Channels of Excitable Membranes. Sinauer Associates Inc.: Sunderland, MA

Hoffman AS (2002) Hydrogels for Biomedical Applications. Advanced Drug Delivery Reviews 43:3-12.

Igelmund P, Fleischmann BK, Fisher IR, Soest J, Gryshchenko O, Bohm-Pinger MM, Sauer H, Liu Q, Jurgen H (1999) Action Potential Propagation Failures in Long-term Recordings from Embryonic Stem Cell-derived Cardiomyocytes in Tissue Culture. European Journal of Physiology 437:669-679.

Jimbo Y, Kawana A, Parodi P, Torre V (2000) The Dynamics of Neuronal Culture of Dissociated Cortical Neurons of Neonatal Rats. Biological Cybernetics 83:1-20.

Kamioka H, Maeda E, Jimbo Y, Robinson HPC, Kawana A (1996) Spontaneous Periodic Synchronized Bursting During Formation of Mature Patterns of Connections in Cortical Neurons. Neuroscience Letters 206:109-112.

Kapur J, Macdonald RL (1997) Rapid Seizure-Induced Reduction of Benzodiazepine and Zn2+ Sensitivity of Hippocampal Dentate Granule Cell GABAa Receptors. The Journal of Neuroscience 17:7532-7540.

Keefer EW, Gramowski A, Gross GW (2001) NMDA Receptor-Dependent Periodic Oscillations in Cultured Spinal Cord Networks. Journal of Neurophysiology 86:3030-3042.

Lelong IH, Petegneif V, Rebel G (1992) Neural Cells Mature Faster of Polyetyleneimine Coated Plates Than on Polylysine Coated Plates. Journal of Neuroscience Research 32:562-568.

Levy RH, Mattson RH, Meldrum BS, Perucca E (2002) Antiepileptic Drugs, 5 Edition. Lippincot, Williams, & Wilkins: Philadelphia, PA.

Luhmann HJ, Prince DA (1991) Postnatal Maturation of the GABAergic System in Rat Neocortex. Journal of Neurophysiology 65:247-263.

Marieb E (1998) Human Anatomy & Physiology, 4 Edition. Benjamin/Cummings Science Publishing: Menlo Park, CA.

Meister M, Pine J, Bayor DA (1994) Multi-neuronal Signals from the Retina: Acquisition and Analysis. Journal of Neuroscience Methods 51:95-106.

Meister M, Wong ROL, Baylor DA, Shatz CJ (1991) Synchronous Bursts of Action Potentials in Ganglion Cells of the Developing Mammalian Retina. Science 252:939-943.

Moorefield SI, Keefer EW, Chapman KD, Gross GW (1999) Drug Evaluations Using Neuronal Networks Cultured on Microelectrode Arrays. Biosensors & Bioelectronics 15:383-396.

Nuttleman CR, Henry SM, Anseth KS (2002) Synthesis and Characterization of Photocrosslinkable, Degradable Poly(vinyl alcohol) –Based Tissue Engineering Scaffolds. Biomaterials 23:3617-3626.

Pine J (1980) Recording Action Potentials from Cultured Neurons with Extracellular Microcircuit Electrodes. Journal of Neuroscience Methods:19-31.

Potter SM, DeMarse TB (2001) A New Approach to Neural Cell Culture for Long Term Studies. Journal of Neuroscience Methods 110:17-24.

Ratner (1996) Biomaterials Science: An Introduction to Materials in Medicine. Academic Press: San Diego, CA.

Razet R, Thomet U, Furtmuller R, Jursky F, Sigel E, Sieghart W, Dodd RH (2000) Use of Bicuculline, a GABA Agaonist, as a Template for the Development of a New Class of Ligands Showing Positive Allosteric Modulation of the GABAa Receptor. Bioorganic & Medicinal Chemistry Letters 10:2579-2583.

Segal MM (1994) Endogenous Bursts Underlie Seizurelike Activity in Solitary Excitatory Hippocampal Neurons in Microcultures. Journal of Neurophysiology 72:1874-1884.

Shahaf G, Marom S (2001) Learning in Networks of Cortical Neurons. The Journal of Neuroscience 21:8782-8788.

Stenger DA, McKenna TM (1994) Enabling Technologies for Cultured Neural Networks. Academic Press: San Diego, CA.

Tateno T, Jimbo Y (1999) Activity-dependent Enhancement in the Reliability of Correlated Spike Timings in Cultured Cortical Neurons. Biological Cybernetics 80:45-55.

Thomas CA, Springer PA, Loeb GE, Berwald-Netter Y, Okun LM (1972) A Miniature Microelectrode Array to Monitor the Bioelectric Activity of Cultured Cells. Exp Cell Res 74:61-66.

Tosney KW, Landmesser LT (1985) Specificity of Early Motorneuron Growth Cone Outgrowth in the Chick Embryo. Journal of Neuroscience 5:2336-2344.

Watanabe S, Jimbo Y, Kamioka H, Kirino Y, Kawana A (1996) Development of Low Magnesium-induced Spontaneous Synchronized Bursting and GABAergic Modulation in Cultured Rat Neocortical Neurons. Neuroscience Letters 210.

BIOGRAPHICAL SKETCH

Alex Cadotte received his B.S. in chemical engineering from Virginia Tech in 1999. He worked in industry from 1999 to 2002 at companies such as General Electric and Corning Optical Fiber in Wilmington, NC. Alex moved to Gainesville, FL, in the Fall of 2002 to pursue a Master of Science at the University of Florida in biomedical engineering specializing in tissue and neural engineering. This thesis is a summary of the work done by Alex under the mentorship of Dr. Thomas DeMarse in this field of study.